Title
Molecular and isotopic partitioning of low-molecular-weight hydrocarbons during migration and gas hydrate precipitation in deposits of a high-flux seepage site

Journal
Chemical Geology, 269(3-4)

ISSN
0167-6695

Authors
Pape, Thomas
Bahr, André
Rethemeyer, Janet
et al.

Publication Date
2010

DOI
10.1016/j.chemgeo.2009.10.009

Chemical Geology 269 (2010) 350–363

Contents lists available at ScienceDirect

Chemical Geology

journal homepage: www.elsevier.com/locate/chemgeo

Molecular and isotopic partitioning of low-molecular-weight hydrocarbons during migration and gas hydrate precipitation in deposits of a high-flux seepage site

Thomas Pape [a,*], André Bahr [a,b], Janet Rethemeyer [c,1], John D. Kessler [d], Heiko Sahling [a], Kai-Uwe Hinrichs [a], Stephan A. Klapp [a], William S. Reeburgh [e], Gerhard Bohrmann [a]

[a] MARUM — Center for Marine Environmental Sciences and Department of Geosciences, University of Bremen, Klagenfurter Strasse, D-28334 Bremen, Germany
[b] IFM-GEOMAR Leibniz-Institute of Marine Sciences, Wischhofstrasse 1-3, D-24148 Kiel, Germany
[c] Alfred Wegener Institute for Polar and Marine Research, Am Handelshafen 12, D-27570 Bremerhaven, Germany
[d] Department of Oceanography, Texas A&M University, College Station, Texas 77843-3146, USA
[e] Department of Earth System Science, University of California Irvine, Irvine CA 92697-3100, USA

ARTICLE INFO

Article history:
Received 5 February 2009
Received in revised form 15 October 2009
Accepted 15 October 2009

Editor: J. Fein

Keywords:
Black Sea
Gas hydrates
Fractionation
Isotopes
Methane radiocarbon
Batumi seep area

ABSTRACT

Detailed knowledge of the extent of post-genetic modifications affecting shallow submarine hydrocarbons fueled from the deep subsurface is fundamental for evaluating source and reservoir properties. We investigated gases from a submarine high-flux seepage site in the anoxic Eastern Black Sea in order to elucidate molecular and isotopic alterations of low-molecular-weight hydrocarbons (LMWHC) associated with upward migration through the sediment and precipitation of shallow gas hydrates. For this, near-surface sediment pressure cores and free gas venting from the seafloor were collected using autoclave technology at the Batumi seep area at 845 m water depth within the gas hydrate stability zone.

Vent gas, gas from pressure core degassing, and from hydrate dissociation were strongly dominated by methane (>99.85 mol.% of $\sum[C_1–C_4, CO_2]$). Molecular ratios of LMWHC ($C_1/[C_2+C_3]>1000$) and stable isotopic compositions of methane ($\delta^{13}C=-53.5‰$ V-PDB; D/H around −175‰ SMOW) indicated predominant microbial methane formation. C_1/C_{2+} ratios and stable isotopic compositions of LMWHC distinguished three gas types prevailing in the seepage area. Vent gas discharged into bottom waters was depleted in methane by >0.03 mol.% ($\sum[C_1–C_4, CO_2]$) relative to the other gas types and the virtual lack of $^{14}C–CH_4$ indicated a negligible input of methane from degradation of fresh organic matter. Of all gas types analyzed, vent gas was least affected by molecular fractionation, thus, its origin from the deep subsurface rather than from decomposing hydrates in near-surface sediments is likely.

As a result of the anaerobic oxidation of methane, LMWHC in pressure cores in top sediments included smaller methane fractions [0.03 mol.% $\sum(C_1–C_4, CO_2)$] than gas released from pressure cores of more deeply buried sediments, where the fraction of methane was maximal due to its preferential incorporation in hydrate lattices. No indications for stable carbon isotopic fractionations of methane during hydrate crystallization from vent gas were found. Enrichments of $^{14}C–CH_4$ (1.4 pMC) in short cores relative to lower abundances (max. 0.6 pMC) in gas from long cores and gas hydrates substantiates recent methanogenesis utilizing modern organic matter deposited in top sediments of this high-flux hydrocarbon seep area.

1. Introduction

Submarine gas hydrate accumulations are widely distributed on continental margins (Judd et al., 2002) and owing to their hydrocarbon storage capacity are of great interest as future energy source. As a consequence of overpressure, a fraction of volatiles can escape from deeply buried gas reservoirs. These volatiles are transported towards the seafloor by diffusive upward migration along concentration gradients or by fluid advection through conduits and can be incorporated into gas hydrates, provided that the percolated sediments are located within the gas hydrate stability zone (GHSZ) and given that methane concentrations in the pore space exceed in situ solubilities (Ginsburg and Soloviev, 1997).

The relative methane partitioning into its major sedimentary pools (dissolved in interstitial waters, as free gas, adsorbed to mineral surfaces, or bound in hydrates) is crucial for an assessment of the methane bioavailability and for calculations of methane budgets and fluxes. However, various parameters, such as concentration of LMWHC, water availability, and temperatures in bottom water and sediment, control the partitioning into subsurface methane pools, which in turn respond highly dynamic to changes in these parameters. For instance Feseker et al. (2009) demonstrated for surface deposits of a Black Sea mud

* Corresponding author. Tel.: +49 421 218 65053; fax: +49 421 218 8664.
E-mail address: tpape@marum.de (T. Pape).
[1] Now at Institute for Geology and Mineralogy, University of Cologne, Zuelpicher Strasse 49a, D-50674 Cologne, Germany.

0009-2541/$ – see front matter © 2009 Elsevier B.V. All rights reserved.
doi:10.1016/j.chemgeo.2009.10.009

volcano that the intensity of advective gas and heat transport from greater depth strongly affects the extent of hydrate formation and decomposition and thus, the amount of hydrate-bound LMWHC.

The molecular and isotopic characteristics of gases generated in deep sediments can be altered during migration and fixation by diverse abiotic and biotic processes. These include i) biological degradation of individual compounds (James and Burns, 1984; Kniemeyer et al., 2007; Larter and di Primio, 2005; Pallasser, 2000), ii) preferential incorporation into hydrate cages (Sloan and Koh, 2007), iii) admixture of secondary volatiles derived from degradation of oil (Milkov and Dzou, 2007; Prinzhofer and Pernaton, 1997; Seewald, 2003), and iv) preferential methane consumption mediated by the anaerobic oxidation of methane (AOM) in top sediments (Barnes and Goldberg, 1976; Hinrichs and Boetius, 2002; Hoehler et al., 1994; Reeburgh, 1976). Considering the different alteration effects associated with upward migration and partitioning, the molecular and isotopic composition of LMWHC in shallow sedimentary pools or in vent gas can deviate from the source gas of the reservoir. Hence, a comprehensive understanding and evaluation of individual processes contributing to post-genetic LMWHC alterations is essential to accurately evaluate the compositions of gas stored in deeply buried reservoirs.

In recent years, studies addressing molecular and isotopic partitioning of LMWHC and carbon dioxide focused mostly on individual processes associated with migration through the sediment or hydrate formation. It follows that comprehensive knowledge of alterations accompanying gas ascending through the GHSZ towards the sediment–water interface is relevant, since these processes additionally control the proportions of individual LMWHC coexisting in the different gas phases (e.g., Pohlman et al., 2005; Sassen et al., 2004). Consequently, molecular partitioning affects the portion of bioavailable LMWHC in near-surface sediments and the water column, where these compounds can serve as substrate for hydrocarbon-degrading microbes.

The Black Sea comprises the world's largest oceanic reservoir of dissolved methane of 96 Tg (Tg = million tons; Reeburgh et al., 1991), which is assumed to be primarily sourced by decomposing gas hydrates and hydrocarbon seeps (Kessler et al., 2006a). Numerous submarine gas emission sites were discovered in the Black Sea, which are often characterized by virulent gas bubble emission into the water column (see Pape et al., 2008 for refs.). The upper boundary of the GHSZ for pure methane hydrate in the Black Sea was calculated to be located around 700 m water depth (Bohrmann et al., 2003; Naudts et al., 2006). Shallow hydrate occurrences were inferred from geophysical data or verified by actual recovery (see Pape et al., 2008 for refs.), occasionally co-occurring with the discharge of bubble forming gas.

To characterize biotic and abiotic alteration processes affecting LMWHC in shallow deposits of a high-flux seep area in the anoxic Eastern Black Sea basin, we sampled near-surface sediment pressure cores, shallow gas hydrates, and vent gas discharged into bottom waters. We report on molecular proportions and isotope compositions of LMWHC and carbon dioxide dissolved in interstitial waters and incorporated in hydrates, which occurred in distinct layers of shallow sediments. The sources of vent gases were emphasized, as well as the origin of hydrate-bound LMWHC, and the molecular and isotopic fractionations associated to hydrate formation. We used a combinatory approach including autoclave sampling in high spatial resolution and sedimentological analysis. These data were complemented by radiocarbon measurements of methane and used to characterize fractionation processes during gas transfer between these sedimentary pools.

2. Geological setting

Active compressional deformation leads to the creation of a W–E trending system of canyons and ridges on the continental slope off Georgia (Klaucke et al., 2006; Meredith and Egan, 2002) in the Black Sea (Fig. 1a). On top of one of such ridges, a high-flux hydrocarbon seepage area, termed 'Batumi seep area' (41°57′N; 41°17′E, Fig. 1b), was recognized in about 840 to 860 m water depth (Klaucke et al., 2006) in the permanently anoxic Black Sea water body. The Batumi seep area is located within the nominal GHSZ for pure methane hydrate, covers a seafloor area of approx. 0.5 km^2 and comprises several sites of focused gas emission. It provides excellent opportunities to study fractionation processes associated with hydrocarbon partitioning, migration and hydrate precipitation, since the co-occurrence of near-surface gas hydrates and gas seepage is documented (Klaucke et al., 2006; Bohrmann et al., 2007). Remotely operate vehicle (ROV)-based video-documentation revealed sea bottom features typically found at sites of focused, high-flux hydrocarbon seepage (e.g., pockmarks, authigenic carbonates forming pavements and chimney-like structures) and a rough micro-topography hints to (sub-)recent gas ebullition (Bohrmann et al., 2007). Seismic profiling showed that individual seepages are related to fluid percolation along vertical faults promoted by diapiric uplift (Wagner-Friedrichs, 2007). A bottom simulating reflector (BSR)-like structure indicated that the base of the GHSZ was in about 150 m below seafloor (bsf). The BSR was interpreted to result from free gas accumulations trapped below the GHSZ (Wagner-Friedrichs, 2007), while the free gas is considered to fuel gas hydrates in overlying strata and individual seafloor seepage sites. LMWHC derived from gravity cores previously taken at that site were interpreted as mixed biogenic and thermogenic gases, implying some input from deeply buried sources (Klaucke et al., 2006).

Active seepage during our recent sampling campaign was indicated by gas flares rising up to about 300 m below sea level (Nikolovska et al., 2008). The authors reported a maximum gas flux of 5.5 $L\,min^{-1}$ from single outlets, and Haeckel et al. (2008) calculated an annual flux of dissolved methane of $2.45 * 10^6$ mol for a field covering 0.31 km^2 of the Batumi seep area. This demonstrates that considerable amounts of LMWHC escape the seafloor at the Batumi seep area within the GHSZ. In general, virulent gas emissions and shallow-buried hydrates classify the area as focused, high gas flux regime (Bhatnagar et al., 2008; Borowski et al., 1996). This classification is corroborated by a maximum penetration of seawater-derived sulfate to the upper decimeters (Haeckel et al., 2008), which is shallow compared to Black Sea non-seep sites (e.g. Aloisi et al., 2004; Jørgensen et al., 2001). Likewise, introduction of methane from seawater into shallow sediments appears quantitatively negligible. Although methane concentrations in bottom waters offshore of Georgia have not been reported so far, they should be less than 15 µM as a background (Kessler et al., 2006a,b), which is far below equilibrium concentration with a hydrate phase in near-surface sediments (93 mM, Haeckel et al., 2008).

3. Materials and methods

A research cruise to the Batumi seep area was conducted in spring 2007 with the R/V METEOR (M72/3, Legs a and b) and the ROV 'QUEST 4000m' of the MARUM, Bremen, within the joint German research project 'METRO'.

3.1. Underwater sampling equipment

Sampling was performed using the winch-operated Dynamic Autoclave Piston Corer (DAPC) and gravity corer, as well as with the Gas Bubble Sampler (GBS), which was handled by the ROV (Figs. 1b and 2b; Table 1). High-precision underwater navigation and positioning of the gear-operated sampling tools was achieved by using an acoustic transponder system (POSIDONIA, IXSEA) mounted on the wire 50 m above the tools.

3.1.1. Dynamic Autoclave Piston Corer

Nine near-surface sediment pressure cores were recovered from the Batumi seep area (Fig. 1b, Table 1) using the Dynamic Autoclave Piston

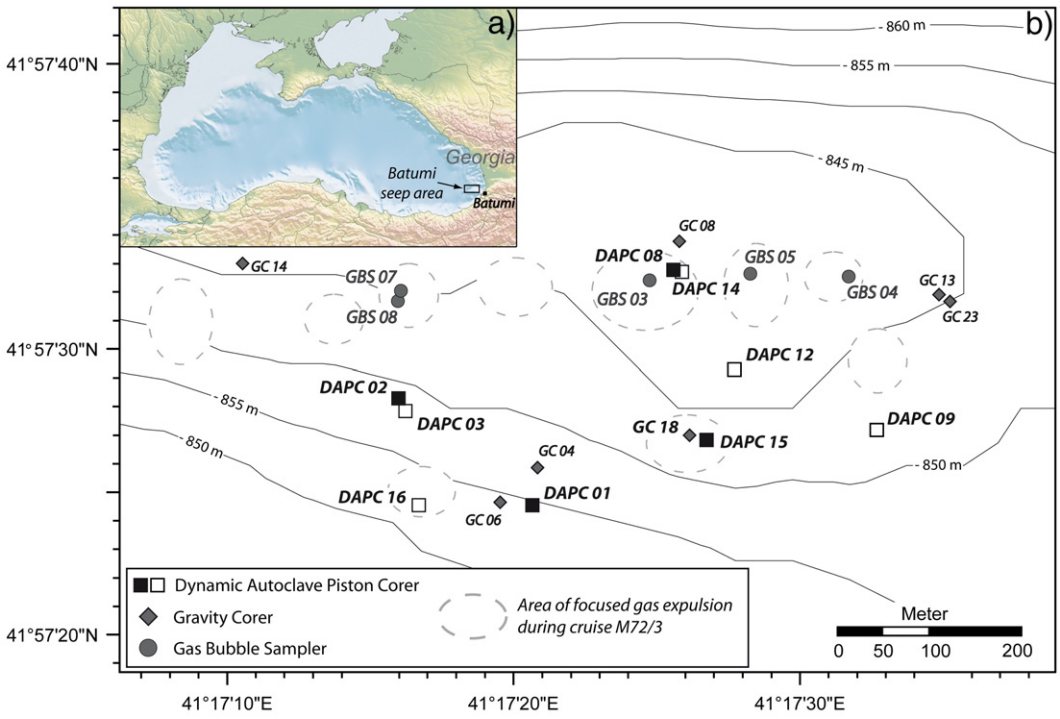

Fig. 1. a) Bathymetric map of the Black Sea showing the position of the Batumi seep area offshore of Georgia. b) Contour map of the Batumi seep area indicating sampling positions of sediment pressure cores and non-pressure gravity cores as well as discharged gas bubbles. Assignments of areas of intense gas expulsion based on hydroacoustic plume imaging (see Bohrmann et al., 2007). DAPC = Dynamic Autoclave Piston Corer; GC = gravity corer, GBS = Gas Bubble Sampler (ROV-based). For DAPC stations, closed symbols indicate cores releasing type IIa_{ds} gas and open squares those releasing type I_{ss} gas (see Section 4.2).

Corer (DAPC, Fig. 2a) housed at the University of Bremen (Abegg et al., 2008). The system is equipped with a core cutting barrel of 265 cm length and a gas-tight pressure chamber, which facilitates preservation of sediment cores at in situ pressure. Immediately upon recovery, the DAPC pressure chamber was connected to a 'gas manifold', which is an assembly of gas-tight valves and valve-activated ports for gas sub-sampling, pressure recording and gas quantification. Release of gas from the pressure chamber, which results in a general pressure decline, was performed incrementally by operating a release port and the overall gas volume was quantified by use of a 'gas catcher' (Heeschen et al., 2007). At selected pressure levels prevailing in the pressure chamber, gas sub-samples were directly taken out of the stream of released gas with a gas-tight syringe, such that only volatiles liberated during core depressurization are collected. The sub-samples were introduced into 20 mL glass

Table 1
List of sediment and gas samples taken at the Batumi seep area during M72/3.

Station no. GeoB	Running no.	Lat. N [°]	Long. E [°]	Water depth [m]	Core recovery [cm]	Pressure upon recovery [bar]
Pressure cores	*DAPC*					
11901	DAPC 01	41:57.410	41:17.344	851	264	68.3
11903	DAPC 02	41:57.472	41:57.266	850	n.d.	72.0
11906	DAPC 03	41:57.465	41:17.270	843	83	64.3
11918	DAPC 08	41:57.547	41:17.427	840	233	84.4
11920	DAPC 09	41:57.454	41:17.545	844	259	71.3
11937	DAPC 12	41:57.489	41:17.462	842	41	49.3
11951	DAPC 14	41:57.546	41:17.431	840	137	80.6
11958	DAPC 15	41:57.448	41:17.446	847	146	87.3
11963	DAPC 16	41:57.410	41:17.278	853	169	27.2
Non-pressure cores	*GC*					
11925	GC 04	41:57.431	41:17.347	844	215	–
11927	GC 06	41:57.410	41:17.324	856	413	–
11936	GC 08	41:57.563	41:17.430	844	193	–
11946	GC 13	41:57.532	41:17.582	842	302	–
11949	GC 14	41:57.550	41:17.175	842	n.d.	–
11956	GC 18	41:57.450	41:17.436	843	96	–
11975	GC 23	41:57.528	41:17.588	844	304	–
Free gas	*GBS*					
11904-16	GBS 03	41:57.541	41:17.413	833	–	78.5
11907-2	GBS 04	41:57.543	41:17.529	834	–	74.8
11907-5	GBS 05	41:57.544	41:17.472	835	–	1.0
11919	GBS 07	41:57.533	41:17.268	833	–	75.0
11921-1	GBS 08	41:57.530	41:17.266	844	–	75.2

DAPC = Dynamic Autoclave Piston Corer; GC = gravity corer; GBS = Gas Bubble Sampler (ROV-based); n.d. = not determined.

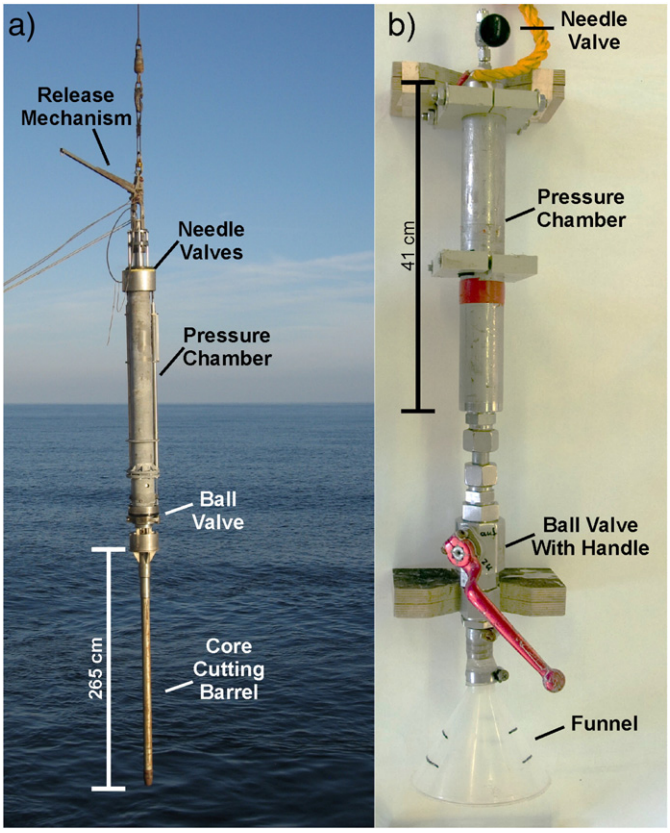

Fig. 2. a) Photograph of the Dynamic Autoclave Piston Corer (DAPC) prior to deployment. b) Photograph of the Gas Bubble Sampler (GBS).

serum vials pre-filled with saturated NaCl solution and sealed with butyl stoppers for i) onboard gas chromatographic analysis and ii) for long-term storage and onshore analysis of carbon and hydrogen isotopic compositions of LMWHC and carbon dioxide and of radiocarbon contents of methane.

3.1.2. Gravity corer

Gas hydrate pieces were recovered at seven stations shown in Fig. 1b using a gravity corer equipped with a 6 m core cutting barrel and plastic hoses as liners for rapid sample access. Immediately upon recovery, hydrates were thoroughly cleaned with ice-cooled purified water, filled into gas-tight syringes, and dissociated at ambient temperature. The released gas was transferred into glass serum vials as described above.

Additionally, we used gravity core GeoB 9922-1 recovered during TTR-15 cruise with R/V Professor Logachev in 2004 from a non-seep site (41°57.25 N; 41°16.70E; 894 m water depth) about 1 km west of the Batumi seep area as a reference.

3.1.3. Gas Bubble Sampler

An in situ pressure Gas Bubble Sampler (GBS, Fig. 2b) was deployed with the ROV manipulator to collect bubble forming vent gas very close to the seafloor above five discrete gas outlets (Fig. 1b). The GBS consists of a steel cylinder (pressure chamber), a valve at the lower end, which is connected to a funnel, and a valve on top. Before deployment, both valves are closed on deck preserving atmospheric pressure inside the GBS. To sample vent gas injected into the water column, gas bubbles are collected in the funnel only a few centimeters above sea ground until the volume of material in the funnel (gas or gas hydrate, traces of seawater) exceeds the capacity of the pressure chamber. By opening the lower valve using the ROV manipulator, the funnel content is sucked into the pressure chamber as a consequence of the pressure difference. Finally, the lower valve is closed again preserving the sample under in situ pressure. After recovery, the upper valve is connected to the 'gas manifold' on deck in order to release collected gas, similar to the DAPC degassing procedure. For samples collected at the Batumi seep area, atmospheric air kept inside the GBS prior to operation contributed 1.2 vol.% in maximum of the overall gas volume released.

3.2. Analytical instrumentation

3.2.1. Total inorganic and total organic carbon

Contents of total carbon and total organic carbon (TOC) were determined by combustion at 1050 °C using a Heraeus CHN-O-Rapid elemental analyzer as described in Müller et al. (1994).

3.2.2. Gas chemical composition

For onboard measurements of chemical compositions, 166 gas sub-samples were analyzed with a two-channel gas chromatograph. C_1 to C_6 alkanes were quantified with a capillary column (OPTIMA-5) connected to a flame ionization detector, whereas O_2, N_2, and CO_2 as well as CH_4 and C_2H_6 were determined using a packed (molecular sieve) stainless steel column coupled to a thermal conductivity detector. Samples were injected on column at room temperature. Calibrations and performance checks of the analytical system were conducted daily using commercial pure gas standards and gas mixtures (Air Liquide, Germany). The analytical error estimated by multiple injections of gas standards was <2.0% for each signal.

All samples were measured within 48 h upon recovery. O_2 and N_2 contributed less than 2 mol.% and represented most likely contaminants introduced during the sub-sampling and analytical procedure. Compositions are given in mol.% assuming $\sum(C_1–C_4\ \text{LMWHC} + CO_2) = 100\%$. Only C_1 to C_4 hydrocarbons were accounted for calculations, since C_{5+} were only found in traces when present.

The molecular ratio R of LMWHC, expressed as C_1/C_{2+} ratio, was calculated according to Eq. (1)

$$R = C_1 / C_{2+} = cC_1 / (cC_2 + cC_3 + cC_4) \quad (1)$$

modified after Bernard et al. (1976), with c = concentration and C_4 = *iso*-C_4 + *n*-C_4.

Gas dryness was calculated using Eq. (2)

$$\text{gas dryness} = cC_1 / \Sigma c(C_1 - C_4) \quad (2)$$

Average proportions (HCp) of individual hydrocarbons and carbon dioxide for the series of gas sub-samples released from sediment pressure cores were calculated according to Eq. (3) given in Heeschen et al. (2007)

$$HCp = \Sigma(HCp_i * (HCv_i - HCv_{i-1})) / \Sigma(HCv_i - HCv_{i-1}) \quad (3)$$

where HCp_i is the portion of the specific compound (%) in each sub-sample (i) and H_{vi} is the accumulated gas volume released when the sub-sample was taken.

3.2.3. Stable isotope ratios ($^{13}C/^{12}C$, D/H)

Stable carbon isotope signatures ($^{13}C/^{12}C$) of C_1 to C_3 hydrocarbons and CO_2 were analyzed for 91 gas sub-samples. Most measurements were carried out at the MARUM (University of Bremen) by GC–isotope ratio mass spectrometry (GC–IRMS) using a Trace GC Ultra (Finnigan) connected via a GC Combustion III line to a DELTA plus XP isotope mass spectrometer (both ThermoFinnigan). For analysis of C_1 and C_2, a CARBOXEN 1006 PLOT fused silica capillary column (Supelco) was used, while C_3 and CO_2 were analyzed using a CP-PoraBOND Q fused silica capillary column (Varian). All samples were injected at room temperature. Chromatography and reproducibility were checked using commercial C_1 to C_6 hydrocarbons standards (SCOTTY 4, Supelco). Moreover, selected samples were analyzed for $^{13}C/^{12}C$ isotopic compositions of methane using a MAT253 IRMS at the IFM-GEOMAR Leibniz-Institute of Marine Sciences, Kiel, Germany, and for $^{13}C/^{12}C$ isotopic compositions of

C_1 to C_3 hydrocarbons and CO_2, as well as D/H of methane according to Dumke et al. (1989) at a commercial lab (Geochemische Analysen, Sehnde, Germany). The reproducibility of stable carbon isotope determinations is estimated at ±0.3‰. All isotopic values are reported in δ-notation in parts permill (‰), relative to the Vienna PeeDee Belemnite (V-PDB) standard for carbon isotopes and to standard mean ocean water (SMOW) for hydrogen isotopes. For comparison, $\delta^{13}C$ values of methane were corrected for statistical offsets, which became obvious for samples representative for all gas types (see Section 4.2) and measured at each of the three laboratories, MARUM, IFM-GEOMAR and the commercial lab.

The carbon isotope fractionation factor $\alpha_C(CO_2–CH_4)$ was calculated using Eq. (4); (Whiticar et al., 1986)

$$\alpha_c(CO_2-CH_4) = (\delta^{13}C-CO_2 + 1000)^*(\delta^{13}C-CH_4 + 1000)^{-1} \quad (4)$$

3.2.4. Radiocarbon concentration of methane

For radiocarbon analysis, eight gas sub-samples were purified and oxidized to CO_2 by combustion using the procedures and apparatus described in Kessler and Reeburgh (2005). The methane-derived CO_2 was converted into graphite by reduction with an excess of hydrogen over an iron catalyst. Radiocarbon concentrations were measured by accelerator mass spectrometry (AMS) in the Keck Carbon Cycle AMS facility at the University of California Irvine. Results are corrected for isotopic fractionation via the simultaneously measured $\delta^{13}C$ value and are reported as percent modern carbon (pMC) with ±1σ measurement uncertainty following the conventions of Stuiver and Polach (1977).

4. Results

4.1. Lithology

Gravity cores and pressure cores from the Batumi seep area generally comprised hemipelagic sediments consisting of finely laminated coccolith ooze (Unit 1; Ross and Degens, 1974) and mid-Holocene sapropel (Unit 2) underlain by late Pleistocene-early Holocene lacustrine mud (Unit 3; Fig. 3). Total thicknesses of the marine units differed strongly indicating considerable variations in the depositional regime of that area for at least the last 8.0 kyrs (Lamy et al., 2006). Gas hydrates were found as isolated, several centimeter-sized massive layers in deeper sections of Unit 2 in three (GC 04, 08, and 18) out of six gravity cores from that area and dispersed in high densities in Unit 3 in all four gravity cores containing this section (GC 06, 08, 13, and 23). Shallowest hydrates were unambiguously present in GC 18 in about 90 cm bsf (Fig. 3) taken in an area of focused gas expulsion (Fig. 1b), but might have been recovered in the core catcher of GC 14, which was bent during sediment penetration.

The TOC depth profile of core GeoB 9922-1 showed values around 2.1% dry weight (dw) in Unit 1 sediments, maximized in 5.6% in the lower part of the sapropelic Unit 2, decreased to about 2.5% at the Unit 2–3 boundary, where it sharply dropped to below 1.0% and remained low at greater depth. TIC in GeoB 9922-1 peaked directly underneath the TOC maximum in Unit 2 sediments (Fig. 3) with 4.7% dw and decreased drastically down to about 1.4% close to the Unit 2–3 boundary. In the upper part of Unit 3 the TIC profile increased with decreasing depth and remained stable in deeper sections with values scattering around 3%.

4.2. Molecular gas composition

Use of multiple sampling tools, i.e., DAPC, gravity corer, and GBS enabled us to collect gases from different near-surface pools (e.g., pressure cores, hydrates, venting free gas) at the Batumi seep area. Average hydrocarbon compositions HCp in gases retrieved from these pools were in general strongly dominated by methane (99.854 to 99.978 mol.% of $\Sigma(C_1–C_4, CO_2)$) followed by ethane (0.014 to 0.047 mol.%; Table 2). Propane, *iso*- and *n*-butane were found in much smaller amounts and C_5- and C_6-derivatives were present only in traces occasionally in vent gas. Carbon dioxide ranged between 0.011 and 0.115 mol.%.

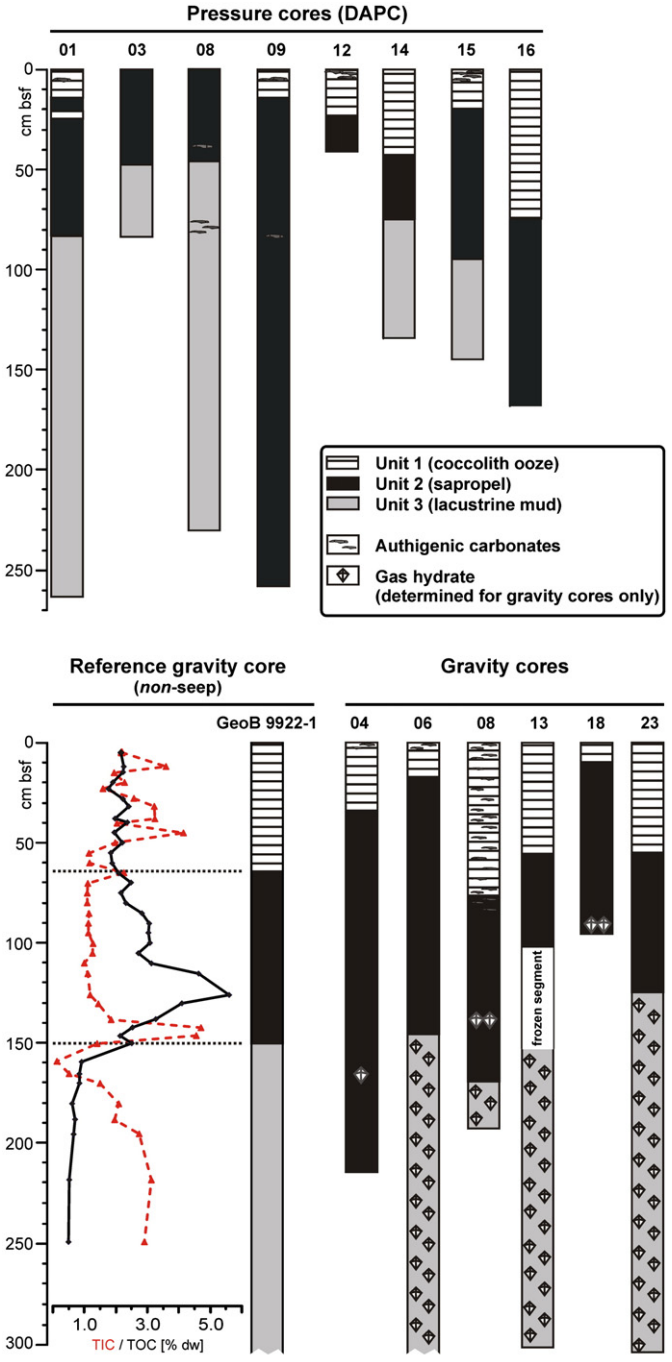

Fig. 3. Lithological compositions of pressure sediment cores (DAPC) and non-pressure (gravity cores) sediment cores recovered from the Batumi seep area. Assignments of lithological units adopted from Ross and Degens (1974). Note: due to technical problems during degassing of DAPC 02 sediment was considerably disturbed. However, DAPC 02 comprised significant portions of Unit 3 material and gas released could be assigned to type II_{ds} gas. For core GC 13 a core segment comprising the Unit 2–Unit 3 transition was deep frozen for subsequent analysis prior to lithological description (data not shown). Depth profiles of TIC-, and TOC-contents compiled for reference core GeoB 9922-1 taken about 1 km W of the Batumi seep area (gas hydrate occurrences not analyzed).

4.3. Stable carbon and hydrogen isotopes of C_1 to C_3 LMWHC and of carbon dioxide

Stable carbon isotopic compositions of methane and ethane were determined for selected gas sub-samples (Table 3). While $\delta^{13}C–CH_4$ values in gas from cores comprising Units 1 and 2 and insignificant portions of Unit 3 (Fig. 3) ranged between −51.7 and −53.0‰, methane from cores

Table 2
Average proportions (HCp) of low-molecular-weight alkanes and CO_2 [in mol.% of $\Sigma(C_1–C_4, CO_2)$] in gas samples from the Batumi seep area.

Station no.	C_1 [mol.%]	C_2 [mol.%]	C_3 [mol.%]	*i*-C_4 [mol.%]	*n*-C_4 [mol.%]	CO_2 [mol.%]	Gas dryness	C_1/C_{2+}	C_1/C_3	C_2/C_3	*i*-C_4/*n*-C_4	Gas type [a]
Sedimentary gas												
DAPC 03	99.9105	0.0474	0.0007	0.0003	n.d.	0.0411	0.9991	2066	144 813	68.7	n.a.	I_{ss}
DAPC 09	99.8541	0.0448	0.0009	n.d.	n.d.	0.1003	0.9985	2189	116 839	52.4	n.a.	I_{ss}
DAPC 12	99.9451	0.0415	0.0014	0.0007	n.d.	0.0114	0.9995	2295	73 896	30.7	n.a.	I_{ss}
DAPC 14	99.9386	0.0427	0.0008	n.d.	n.d.	0.0179	0.9994	2297	119 153	50.9	n.a.	I_{ss}
DAPC 16	99.9285	0.0533	0.0009	n.d.	n.d.	0.0173	0.9993	1845	117 517	62.7	n.a.	I_{ss}
Mean	**99.9154**	**0.0459**	**0.0009**	**0.0002**	**n.d.**	**0.0376**	**0.9992**	**2139**	**108 932**	**50.1**		
DAPC 01	99.9369	0.0337	0.0007	n.d.	n.d.	0.0287	0.9994	2907	141 550	47.7	n.a.	IIa_{ds}
DAPC 02	99.9585	0.0291	0.0011	0.0003	n.d.	0.0109	0.9996	3274	92 602	27.0	n.a.	IIa_{ds}
DAPC 08	99.9380	0.0295	0.0012	n.d.	n.d.	0.0313	0.9994	3254	85 597	25.3	n.a.	IIa_{ds}
DAPC 15	99.9507	0.0330	0.0009	n.d.	n.d.	0.0154	0.9995	2945	110 186	36.4	n.a.	IIa_{ds}
Mean	**99.9460**	**0.0313**	**0.0010**	**0.0001**	**n.d.**	**0.0216**	**0.9995**	**3095**	**103 568**	**32.5**		
Vent gas												
GBS 03	99.8576	0.0192	0.0059	0.0018	0.0006	0.1149	0.9986	3633	16 963	3.3	2.8	IIb_{vg}
GBS 04	99.8666	0.0144	0.0033	0.0008	n.d.	0.1149	0.9987	5383	30 096	4.4	n.a.	IIb_{vg}
GBS 05	99.8876	0.0221	0.0038	0.0012	n.d.	0.0852	0.9989	3671	26 041	5.8	n.a.	IIb_{vg}
GBS 07	99.9171	0.0205	0.0029	0.0009	0.0006	0.0580	0.9992	4019	34 753	7.1	1.4	IIb_{vg}
GBS 08	99.9784	0.0183	0.0023	0.0009	n.d.	0.0000	0.9998	4631	42 800	7.8	n.a.	IIb_{vg}
Mean	**99.9015**	**0.0189**	**0.0037**	**0.0011**	**0.0002**	**0.0746**	**0.9990**	**4267**	**27 367**	**5.2**		
Hydrate-bound gas												
GC 14	99.8995	0.0423	0.0008	n.d.	n.d.	0.0575	0.9990	2318	121 633	51.5	n.a.	I
GC 04	99.9331	0.0237	0.0018	n.d.	n.d.	0.0414	0.9993	3920	56 161	13.3	n.a.	IIb
GC 13	99.9416	0.0226	0.0012	n.d.	n.d.	0.0347	0.9994	4212	85 158	19.2	n.a.	IIb
GC 06	99.9425	0.0287	0.0013	n.d.	n.d.	0.0274	0.9994	3323	74 613	21.5	n.a.	IIa_{gh}
GC 08	99.9427	0.0317	0.0010	n.d.	n.d.	0.0246	0.9994	3058	98 701	31.3	n.a.	IIa_{gh}
GC 18	99.9512	0.0274	0.0010	n.d.	n.d.	0.0203	0.9995	3509	95 322	26.2	n.a.	IIa_{gh}
GC 23	99.9214	0.0331	0.0009	n.d.	n.d.	0.0446	0.9992	2944	114 984	38.1	n.a.	IIa_{gh}
Mean	**99.9394**	**0.0302**	**0.0011**	**n.d.**	**n.d.**	**0.0292**	**0.9994**	**3209**	**95 905**	**29.3**		

Molecular proportions of individual compounds given for DAPC and GBS gases are mean values calculated for the series of sub-samples.
Type I_{ss} gas: $C_1/C_{2+} < 2350$; type IIa (ds/gh): $2900 < C_1/C_{2+} < 3550$; IIb_{vg} gas $C_1/C_{2+} > 3600$.
n.d. = not detected; n.a. = not analyzed.
[a] According to molecular composition.

comprising larger fractions of Unit 3, from decomposing hydrates, and from bubble forming vent gas was slightly enriched in ^{13}C with $\delta^{13}C$ values of −51.0 to −52.0‰. $\delta^{13}C$ values scattered from −36.8 to −39.2‰ for ethane and between −25.7 and −29.1‰ for propane, respectively. $\delta^{13}C$–CO_2 ranged between −9.4 and −19.6‰ with most negative values found for carbon dioxide in vent gas. δD–CH_4 values determined for selected sub-samples retrieved with the DAPC, the GBS and from decomposing gas hydrates ranged between −152 and −190‰ (Fig. 5c).

4.4. Radiocarbon concentrations of methane

Vent gas-derived methane contained lowest ^{14}C concentrations of <0.09 pMC, while intermediate values of up to 0.6 pMC characterized type IIa_{GH} gas (Fig. 6). Highest concentrations of modern carbon with up to 1.4 pMC were measured for methane contained in pressure cores devoid of substantial amounts of Unit 3.

4.5. Pressure loss and quality of gas samples

For three out of nine pressure cores, recovery pressure was close to the hydrostatic pressure (ca. 84 bar; Table 1). Except for DAPC 01, 03, 12, and 16, recovery pressure was preserved within the GHSZ. Because the top of the DAPC pressure chamber is sealed with a piston (Abegg et al., 2008), which is connected to the ship's wire and carries the entire DAPC, loss of pressure is most likely due to loss of small amounts of water through leakages of the ball valve at the lower end (Fig. 2a). Moreover, as no correlation between gas composition (Table 2) and recovery pressure was found, the composition of sedimentary gas does not seem to be significantly affected by leakages.

For four out of five GBS deployments, recovery pressure was in maximum 8.6 bar below hydrostatic pressure (Table 1). The only exception, GBS 05, lost pressure nearly completely. Although molecular fractionation could not be excluded in principle with respect to gas leakage during GBS recovery, LMWHC compositions of all vent gas samples are similar and different from gas of the other gas pools (Table 2). Consequently, the DAPC and GBS provided gas samples of excellent quality mostly unaffected by molecular and isotopic fractionations, which might occur when conventional sampling systems are used and samples are subject to extreme degassing during recovery.

5. Discussion

Comprehensive gas chemical analysis in conjunction with lithological core descriptions provided meaningful information on sources of individual low-molecular-weight hydrocarbons (LMWHC) and carbon dioxide in shallow deposits of the Batumi seep area, as well as their partitioning into different sedimentary pools during ascent from deep subsurface reservoirs. For the different gas pools, the gases exhibit small but diagnostic differences in their LMWHC and carbon dioxide distribution patterns. Indications for alterations of molecular and isotopic compositions of the gas samples due to different sampling procedures from the gas pools did not become evident.

In the following, major sources of volatiles in the subsurface and the effects of post-genetic alterations induced during migration through deeper sediments, hydrate crystallization, and passage through top sediments are discussed. Finally, we aim to clarify the relevance of biotic and/or abiotic modifications on the composition of gases in the individual pools.

5.1. Primary sources of LMWHC and carbon dioxide

Two principal processes – microbial conversion of low-molecular-weight organic substrates and thermocatalytic degradation of organic

Table 3
Stable hydrogen isotopic composition and radiocarbon concentration of methane, stable carbon isotopic compositions of hydrocarbons and carbon dioxide, carbon isotope separations (Whiticar, 1999) of several pairs of volatiles, and carbon isotope fractionation factor $\alpha_C(CO_2–CH_4)$.

Station no.	Gas type	$\delta^{13}C–C_1$[a] [‰ V-PDB]	$\delta^{13}C–C_2$[a] [‰ V-PDB]	$\delta^{13}C–C_3$ [‰ V-PDB]	$\delta^{13}C–CO_2$[a] [‰ V-PDB]	$\Delta\delta^{13}C$ ($C_2–C_1$) [‰ V-PDB]	$\Delta\delta^{13}C$ ($C_3–C_2$) [‰ V-PDB]	$\Delta\delta^{13}C$ ($CO_2–C_1$) [‰ V-PDB]	$\alpha c(CO_2\text{-}CH_4)$
Sedimentary gas									
DAPC 03	I_{ss}	−52.3 ± 0.2	−38.6 ± 1.1		−10.3	13.7		42.0	1.044
DAPC 09	I_{ss}	−52.2 ± 0.3	−39.1 ± 0.7	−25.9	−10.0	13.1	13.2	42.2	1.045
DAPC 14	I_{ss}	−52.0 ± 0.3	−37.4 ± 1.4	−25.7	−12.2	14.6	11.7	39.8	1.042
		−52.2	−38.4	−25.8	−10.8	13.8	12.6	41.9	1.044
DAPC 01	IIa_{ds}	−51.3 ± 0.2	−38.6 ± 1.0	−27.9	−9.9	12.7	10.7	41.4	1.044
DAPC 08	IIa_{ds}	−51.7 ± 0.3	−38.9 ± 0.8	−27.8	−11.3	12.8	11.1	40.4	1.043
		−51.5	−38.8	−27.9	−10.6	12.8	10.9	40.9	1.043
Vent gas									
GBS 03	IIb_{vg}	−51.3	−38.8	−29.1	−19.6	12.5	9.7	31.7	1.033
GBS 04	IIb_{vg}	−51.2	−38.6		−13.7	12.6		37.5	1.040
GBS 05	IIb_{vg}	−51.0	−39.2		−13.8	11.8		37.3	1.039
GBS 07	IIb_{vg}	−51.2	−38.6	−28.1	−17.7	12.6	10.5	33.5	1.035
GBS 08	IIb_{vg}	−51.5	−38.4		−17.8	13.1		33.7	1.036
		−51.2	−38.7	−28.6	−16.5	12.5	10.1	34.7	1.037
Hydrate-bound gas									
GC 14	I	−51.5		−26.1	−9.5			42.0	1.044
GC 04	IIb	−50.9	−36.8			14.1			
GC 06	IIa	−50.5							
GC 08	IIa	−51.7	−37.0	−27.0	−10.9	14.7	10.0	40.8	1.043
GC 13	IIb	−50.2	−38.1	−27.8	−9.4	12.1	10.3	40.8	1.043
GC 18	IIa	−50.3	−37.6			12.7			
GC 23	IIa	−51.2	−38.4		−10.4	12.8		40.8	1.043
		−50.8	−37.6	−27.4	−10.2	13.2	10.4	40.6	1.043

[a] Mean value calculated for isotopic compositions determined for selected sub-samples retrieved during degassing; values determined for individual sub-samples are illustrated in Fig. 5b.

matter – are considered to lead to generation of primary LMWHC in the Black Sea subsurface (Pape et al., 2008). Commonly, several combinations of molecular and isotopic characteristics are used to assign the deep subsurface sources of LMWHC and their post-genetic alterations (Bernard et al., 1976; Schoell, 1988; Whiticar, 1999). As we aimed to ascertain even small-scale molecular and isotopic modifications of LMWHC and carbon dioxide during gas migration and to get a detailed knowledge of their sources, we investigated several gas chemical parameters. C_1/C_{2+} ratios (Table 2; Fig. 5a), the very low abundances or absence of *n*-C_4 and higher homologues (Table 2; Claypool and Kvenvolden, 1983) as well as dryness indices (Table 2; Schoell 1980) suggest that a significant portion of methane in all gas types retrieved from the Batumi seep area is of microbial origin. However, combining C_1/C_{2+} ratios and $\delta^{13}C–CH_4$ values, the gases plot beyond the fields representative for the principal LMWHC sources (Fig. 5a and c). A contribution of thermogenic (^{13}C-enriched) LMWHC and carbon dioxide is inferred from the $\delta^{13}C–CH_4$ vs. $\delta D–CH_4$ relationship (Fig. 5c), $\delta^{13}C–C_2H_6$ values (Table 3; Fig. 5d); $\delta^{13}C–CO_2$ values (Table 3), the $\delta^{13}C–CH_4$ vs. $\delta^{13}C–CO_2$ relationship (Table 3), as well as stable carbon isotope separations between individual pairs of C_1 to C_3 alkanes (Table 3; Clayton, 1998; Milkov, 2005; Pallasser, 2000; Scott et al., 1994; Schoell, 1983; Schoell 1988). Taking all data into account, we conclude that the major fraction of methane originates from microbial formation while a less important methane fraction as well as the majority of higher homologues is provided by thermocatalytic production.

$^{13}C/^{12}C$ and D/H isotopic ratios of methane suggest that microbial carbonate reduction using hydrogen is the primary process of methanogenesis in the deep Batumi subsurface (Fig. 5c; Rice and Claypool, 1981; Schoell, 1983; Schoell, 1988). However, $CO_2–CH_4$ isotopic fractionation factors α_c between 1.033 and 1.040 calculated for the vent gas (Table 3) are smaller than those attributed to bicarbonate-based methanogenesis in marine systems (>1.05, Whiticar et al., 1986). This is possibly due to the mixing of thermogenic methane enriched in ^{13}C (Jones et al., 2008; Larter and di Primio, 2005; Milkov and Dzou, 2007; Seewald, 2003) or microbial methane oxidation. For sulfate-free sediments, AOM has been shown to base on diverse electron acceptors, such as nitrite, nitrate, iron or manganese (Raghoebarsing et al., 2006; Beal et al., 2009).

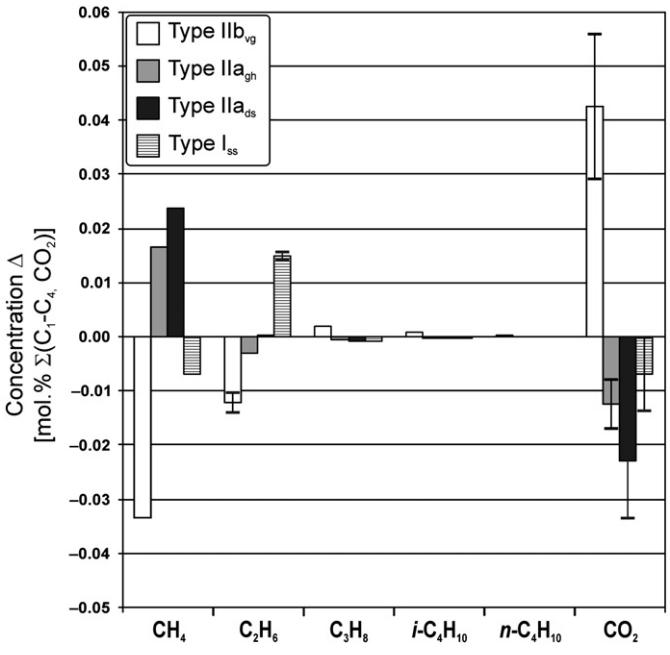

Fig. 4. Bar diagram depicting relative differences in the molecular compositions of C_1 to *n*-C_4 LMWHC and CO_2 in samples from the different gas reservoirs. Concentrations are given as difference between individual gas types and an arithmetic average calculated using type specific mean values. Type specific values are mean values of all samples recovered with the respective tool, except for DAPC types I and II. Type IIa_{ds} gas was retrieved from cores containing amounts of Unit 3 sediments, while cores releasing type I_{ss} gas comprised no or insignificant amounts of Unit 3. Note: Error bars are only given for values exceeding thickness of symbol line.

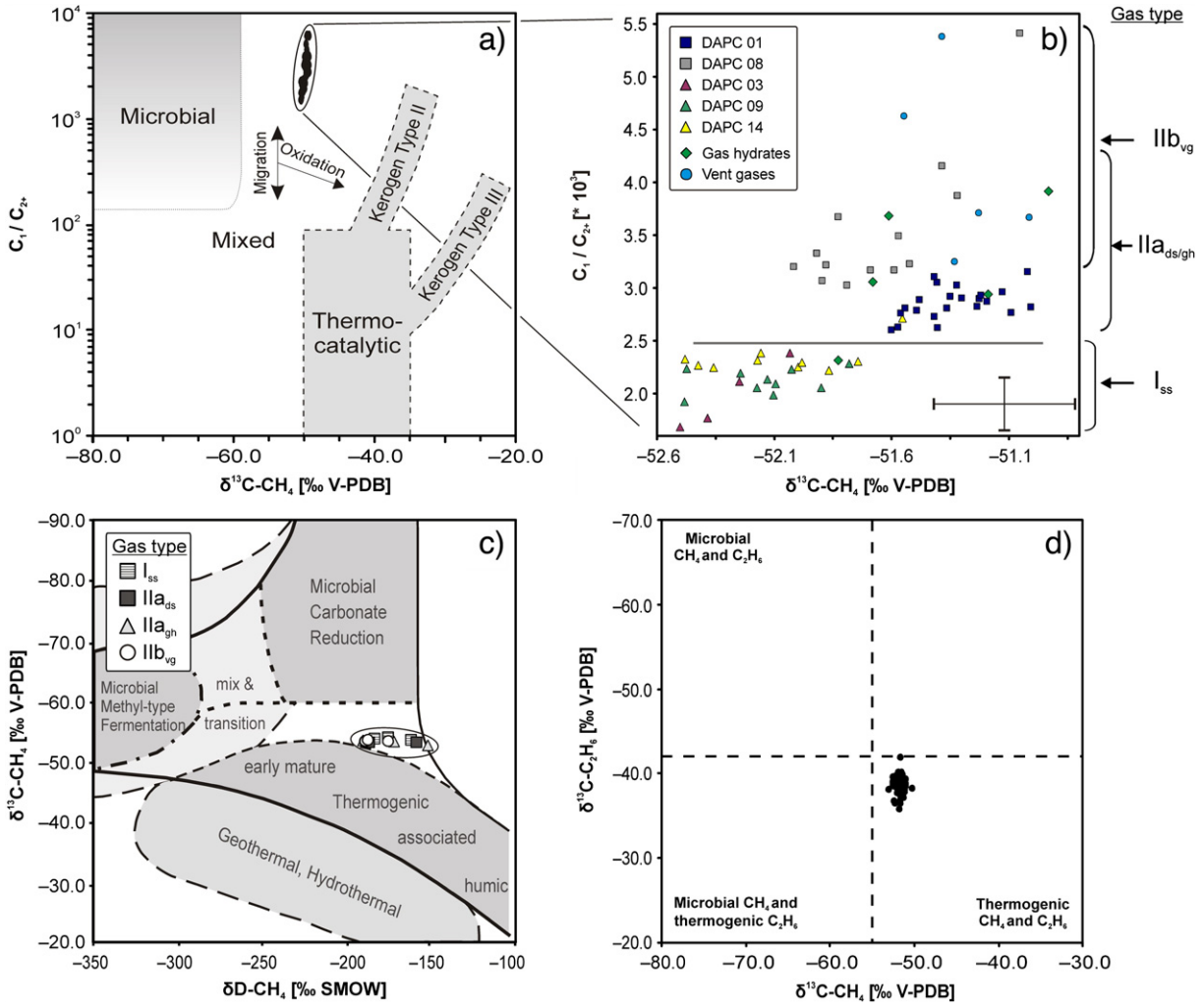

Fig. 5. a) 'Bernard diagram' modified after Whiticar (1989) showing $\delta^{13}C$ values of methane vs. molecular hydrocarbon ratios. b) Close up of the 'Bernard diagram' (Bernard et al., 1976) illustrating trends of $\delta^{13}C$–CH_4 values for type I and type II gases. The line indicates a transition value for $C_1/C_{2+} \approx 2500$ which was found to separate type I and type II gases (see also Table 1) Error bars indicating standard deviations are given in the lower right corner. c) Cross plot of $\delta^{13}C$ values vs. $\delta^{2}H$ values of methane in selected sub-samples representing different gas types (classification adopted from Whiticar, 1999). d) Cross plot of $\delta^{13}C$–CH_4 vs. $\delta^{13}C$–C_2H_6 illustrating main sources of methane and ethane in Batumi seep gases (classification adopted from Milkov, 2005). Note: error bars for ^{13}C values are in size similar to the symbols.

Irrespective of post-genetic alterations, C_1/C_2 and C_2/C_3 ratios, $\delta^{13}C$ values of methane, ethane and carbon dioxide as well as gas dryness indices suggest that thermogenic constituents of the vent gas are sourced from immature to early mature kerogen of the sapropelic, marine type II (Rice and Claypool, 1981; Rooney et al., 1995; Whiticar, 1989; Whiticar, 1999) and/or from secondary production due to oil cracking (Milkov and Dzou, 2007; Prinzhofer and Huc, 1995; Seewald, 2003). $\delta^{13}C$–CO_2 values likewise suggest that carbon dioxide in the vent gas primarily originates from the degradation of kerogen and soluble organic matter (Dai et al., 1996; Irwin et al., 1977; Wycherley et al., 1999). A potential source rock for primary gas formation is the Late Oligocene–Lower Miocene Maikop series, which comprises significant amounts of type II kerogen (Efendiyeva, 2004), and is located at 1–4 km depth in the Eastern Black Sea (Banks et al., 1997; Meredith and Egan, 2002). In addition, the Maikopian formation is known to favor oil formation (Efendiyeva, 2004; Inan et al., 1997), and oil seepage was documented at several sites close to the Batumi seep area (Bohrmann et al., 2007).

The depth range of the major gas generation remains uncertain. Radiocarbon data (Table 3) substantiate that the carbon source of vent gas methane is in principle older than about 50 kyrs. Nonetheless, individual proportions of microbial and thermogenic LMWHC might be generated in different depths prior to mixing. Assuming a geothermal gradient of 0.03 °C m^{-1} and given that the maximum temperature tolerated by prokaryotes including methanogenic archaea is about 90 °C (Orphan et al., 2000; Valentine et al., 2004), microbial methane is formed at burial depths of less than about 2.7 km bsf. In contrast, LMWHC from type II kerogens or oil cracking are typically generated at temperatures exceeding 100 °C (Clayton, 1991) implying a minimum formation depth of 3.0 km bsf for the thermogenic LMWHC present in gases from the Batumi seep area.

Although differences in the molecular and isotopic properties were generally small for gas from the different shallow reservoirs at the Batumi seep area, measurement of a number of representative samples revealed clear trends. These allowed for classification of different gas types. In the following, abbreviations are used for the gas types representative for the major gas pools, namely I_{ss} (shallow sedimentary, DAPC), IIa (deep sedimentary, DAPC; gas hydrates, gravity corer), and IIb_{vg} (vent gas, GBS). In addition, type IIa gas is assigned as type IIa_{ds} (deep sedimentary) and type IIa_{gh} (gas hydrates) gas, respectively, unless it is meant unspecifically. Type I_{ss} gas is most distinct in composition relative to the other gas types as it is characterized by a relative depletion in methane ($C_1/C_{2+} < 2350$; Table 2) compared to gas falling into type IIa ($2900 < C_1/C_{2+} < 3550$) and IIb_{vg} ($C_1/C_{2+} > 3600$). Except for DAPC 03 and 14 which contained some Unit 3 material, type I_{ss} gas was retrieved from pressure cores confined to Units 1 and 2 (DAPC 09, 12, 16) and from one hydrate piece (GC 14), which clogged the core catcher. The compositions of LMWHC released from nearly all pressure cores comprising Unit 3 (DAPC 01, 02, 08, and 15) and from the majority of decomposing hydrates (GC 06, 08, 18, and 23)

were typified as type IIa gas. The presence of individual gas types in distinct sediment depth intervals becomes particularly obvious when comparing gas compositions of cores DAPC 08 (type IIa_{ds}) and 14 (type I_{ss}), which were located very close to each other (Fig. 1b), but differed in penetration depth (Fig. 3; Table 3), LMWHC composition (Table 2), and $\delta^{13}C$ and ^{14}C content of methane (Fig. 6), respectively. As C_1/C_{2+} ratios of type I_{ss} and type IIa_{ds} gases are separated from each other and intermediate values were found for only a few gas sub-samples taken during core degassing, concentrations of type I_{ss} gas (shallow sediments) should be much lower than those of type IIa_{ds} gas (including deeper, hydrate-bearing sediments). This supports preferential hydrate accumulations below Unit 2. Type IIb_{vg} gas includes both, gas venting into bottom waters as well as hydrate-bound gas (GC 04, 13) and is more closely related to type IIa gas.

More specifically, type I_{ss} gas was not only depleted in methane, but also enriched in ethane compared to the arithmetic average calculated for the four gas types (Fig. 4). Type IIa_{ds} and IIb_{vg} gases are distinguished by methane and ethane with both compounds being depleted in the latter compared to average values. In contrast, propane, C_4-homologues, and carbon dioxide were comparably enriched in type IIb_{vg} gas. *iso*- and/or *n*-C_4 alkanes were close to the detection limit in type IIa_{gh} gas, but always detected in type IIb_{vg}. Largest fractions of carbon dioxide were found in type IIb_{vg} gas, followed by type I_{ss} and type IIa_{ds} gas. Methane in vent gas (type IIb_{vg}) was slightly enriched in ^{13}C compared to type IIa and I_{ss} gas (Table 3).

An important goal of this study was to clarify whether gas venting from the seafloor at the Batumi seep area is fueled by decomposing hydrates in near-surface sediments or by deep subsurface reservoirs. Average molecular compositions of the individual gas types demonstrate that vent gas is relatively depleted in methane and ethane, but enriched in wet gas LMWHC (C_3 and *n*-C_{4+}; Table 2; Fig. 4), attributed to admixture of gas from thermocatalytic processes (Fig. 5a and c; Claypool and Kvenvolden, 1983; Schoell, 1983). Propane and carbon dioxide in vent gas show strongest ^{13}C-depletions compared to those in hydrate-bound gas (Table 3). Furthermore, in contrast to that in other gas types, vent gas-derived methane is virtually radiocarbon-free (Fig. 6), proving that its formation is based on fossil organic carbon. Thus, the majority of bubble forming vent gas appears to be directly sourced from deep subsurface reservoirs and to bypass the shallow gas hydrate pool. Similar conclusions were drawn for the origin of vent gas at seep areas in the Gulf of Mexico (Sassen et al., 2003, 2004), or on the Cascadia Margin (Pohlman et al., 2005).

Accordingly, volatiles from decomposing hydrates seem currently to contribute only small gas amounts to bubble forming vent gas at the Batumi seep area. This conclusion is supported by the calculated gas hydrate stability (Fig. 7), as gas hydrates are 14 bar or almost 1.6 °C, respectively, below decomposition conditions. Moreover, supply of vent gas from deep reservoirs through vertical faults (Wagner-Friedrichs, 2007) appears plausible with respect to the seepage intensity observed (Nikolovska et al., 2008). Assuming that transport of vent gas through permeable conduits proceeds with high velocity and low residence time compared to diffusive transport, LMWHC and carbon dioxide of this gas type should only be slightly affected by syn-migration alterations. Thus, the composition of vent gas associated with high fluid outflow might resemble that of gas in its subsurface reservoir.

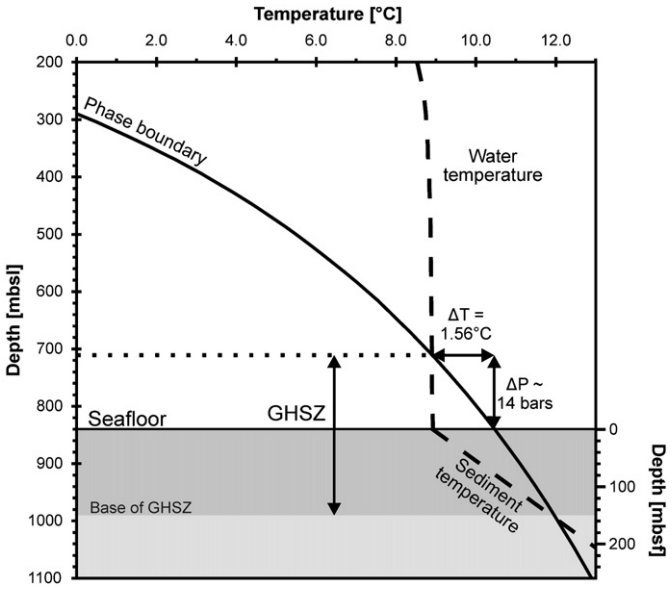

Fig. 7. Phase boundaries of the nominal gas hydrate stability zone (GHSZ) calculated for gas hydrate structure I at the Batumi seep area using bottom water salinity (20.97), temperature (8.96 °C), and pressure, respectively, and gas chemical data obtained in March/April 2007. Phase boundaries were calculated using the software package provided by Sloan and Koh (2007). Calculations using individual LMWHC and CO_2 compositions measured for the different gas types (type I, IIa, and IIb) revealed negligible deviations from the general phase boundary depicted.

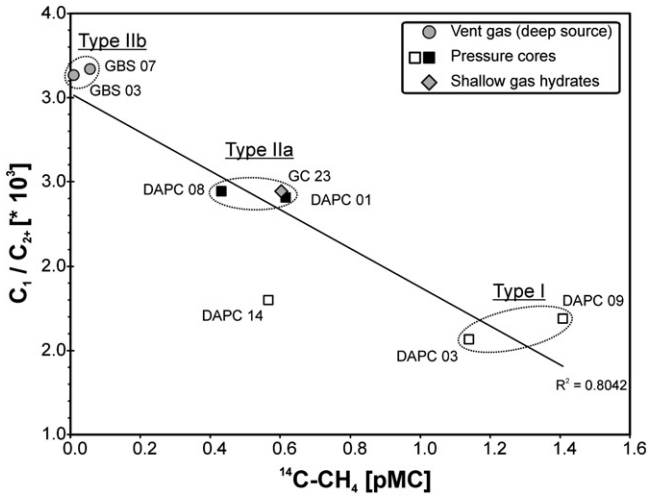

Fig. 6. Cross plot illustrating ^{14}C concentrations of methane in the different gas types. Note: error bars for ^{14}C values are in size similar to the symbols.

5.2. Alterations of LMWHC and carbon dioxide

Different C_1/C_{2+} ratios characterizing gas types in individual shallow gas reservoirs at hydrate-bearing sites result from molecular partitioning into different sedimentary pools during passage through the sediment (Prinzhofer and Pernaton, 1997; Schoell, 1983), fractionation during hydrate formation (Milkov et al., 2004; Sassen et al., 2000; Sloan and Koh, 2007), and/or molecular alteration due to preferential microbial consumption (James and Burns, 1984). Our results show that such processes also happen in the subsurface of the Batumi seep area.

5.2.1. Abiotic alterations associated with gas hydrate precipitation

As proposed in Section 5.1, hydrates at the Batumi seep area typically do not precipitate from type I_{ss} gas. Nevertheless, hydrate-bound methane (type IIa_{gh}) is slightly enriched in ^{13}C compared to

Similar molecular distributions and $\delta^{13}C$–CH_4 values (Figs. 4 and 5b, Tables 2 and 3) support the idea that hydrate-bound volatiles are primarily sourced by vent gas (type IIb_{vg}). Vent gas fueling hydrate was also proposed for shallow hydrates at the Cascadia margin (Haeckel et al., 2004). Surprisingly, hydrate-bound methane in GC 23 recovered from Unit 3 material and type IIa_{ds} gas contained small amounts of radiocarbon corresponding to a conventional ^{14}C age of 41 kyrs B.P. This demonstrates that vent gas is not the exclusive source of LMWHC bound in near-surface hydrates at the Batumi seep area.

that in type IIa_{ds} gas, pointing to some contributions of methane from type I_{ss} gas in pressure cores containing Unit 3 deposits. Intrusion of type I_{ss} gas might have also infiltrated amounts of radiocarbon–methane in type IIa_{ds} gas and a hydrate piece (Fig. 6).

Differences in the molecular compositions of all type II gases are small when compared to type I_{ss} gas, i.e., the composition of all type II gases resembles that of gas incorporated in structure I (sI; see Section 5.3) gas hydrate. These characteristics suggest either that the molecular composition of gas in deeper reservoirs sourcing the vent gas meets the requirements for sI hydrate formation in shallow sediments to a large extent, or that molecular fractionation of substantial gas portions by sI hydrate formation and subsequent heat-induced dissolution takes place at greater depths (e.g., Suess et al., 1999). Molecular fractionations between vent gas and hydrates are substantiated, as samples including hydrate-bound gas (type IIa_{ds}, type IIa_{gh}) are comparably enriched in methane and ethane, depleted in propane and carbon dioxide, and are virtually devoid of *iso*-butane and *n*-butane (Fig. 4). Similar molecular distinctions observed at different hydrate-bearing sites (e.g., Charlou et al., 2007; Milkov, 2005; Milkov et al., 2004; Sassen et al., 2000; Sloan and Koh, 2007) were attributed to size exclusion during hydrate crystallization. In contrast, significant differences in the molecular compositions found for type I_{ss} and type IIa gas are mainly attributed to microbial transformation (see Section 5.2.2).

The differences in $\delta^{13}C$ values of methane, ethane as well as D/H of methane between vent gas (type IIb_{vg}) and type IIa gases were insignificant and did not give evidence for notable isotope fractionation of LMWHC during hydrate incorporation (Table 3; Fig. 5a–d). The lack of significant carbon isotopic fractionations of methane during hydrate crystallization from vent gas was already reported from sites at the Gulf of Mexico continental slope (Brooks et al., 1986; Sassen et al., 1999; Sassen et al., 2001; Sassen et al., 2004) and in the Sea of Marmara (Bourry et al., 2009). As ^{13}C-enrichments of carbon dioxide were observed for all gas types relative to vent gas (Table 3), the $^{13}C/^{12}C$ isotopic fractionation of carbon dioxide does not seem to be directly linked to hydrate precipitation.

5.2.2. Biological alterations

5.2.2.1. Biological conversion of non-methane LMWHC and carbon dioxide. The molecular composition of shallow gas (type I_{ss}) at the Batumi seep area is likely influenced by molecular fractionation associated with hydrate crystallization. After release by hydrate dissociation, LMWHC tend to ascend towards the seawater-penetrated near-surface sediments, where they are affected by microbial metabolic processes. Highest relative proportions of C_4 LMWHC, which are commonly considered as by-product of thermocatalytic organic matter degradation (Claypool and Kvenvolden, 1983), were present in vent gas (Table 2; Fig. 4). However, from the $\delta^{13}C$-values of methane and ethane we anticipated the presence of significant amounts of LMWHC$\geq C_2$ also in the sedimentary gas types (IIa_{ds} and I_{ss}; see Section 5.1). These findings could be explained by i) exclusion of C_{3+} LMWHC during hydrate precipitation; ii) minor contributions of thermogenic LMWHC but significant input of secondary methane relatively enriched in ^{13}C, and/or iii) removal of thermogenic C_{4+} LMWHC by biodegradation. Exclusion of C_{3+} LMWHC from hydrates is substantiated as all hydrate pieces lacked C_4 LMWHC. Admixture of secondary methane, however, appears ambiguous for Batumi seep gases based on our data set. Secondary methane is released by the biodegradation of hydrocarbons and other organic compounds occurring in sediment intervals spanning from deep reservoirs to the surface (Head et al., 2003; Milkov and Dzou, 2007; Pallasser, 2000; Scott et al., 1994; Seewald, 2003) and was assumed to occur in mud volcano deposits in the Sorokin Trough in the Northeastern Black Sea (Blinova et al., 2003; Stadnitskaia et al., 2008).

In contrast, microbial degradation of non-methane LMWHC could be demonstrated for the gases at the Batumi seep area. This process is considered to preferentially attack LMWHC with secondary carbon atoms in sub-terminal positions relative to those with tertiary or quaternary sub-terminal carbons (Boreham et al., 2008). Hence, C_3, and linear C_4 and C_5-alkanes are typically transformed by hydrocarbon degraders, whereas C_2 and *iso*-C_4 appear to be less affected or even remain unaltered (Head et al., 2003; Horstad and Larter, 1997; James and Burns, 1984; Kniemeyer et al., 2007; Larter and di Primio, 2005; Stadnitskaia et al., 2006). Typically, anaerobic microbial degradation of wet gas LMWHC (C_{2+}) by electron acceptors other than sulfate (Widdel and Rabus, 2001; Zengler et al., 1999) leads to addition of ^{13}C-enriched, secondary methane (Milkov and Dzou, 2007).

The *iso*-butane over *n*-butane prevalence (1.4 and 2.8) determined for vent gas from two stations (GBS 03 and 07; Table 2) points to microbial LMWHC alteration (James and Burns, 1984) in the gas reservoir and/or during ascent (as *n*-C_4 was absent in all gases from pressure cores and gas hydrates) from below. Indications for microbial consumption of propane, i.e., considerable removal accompanied by slight ^{13}C-enrichments of the residual propane in type I_{ss} and type IIa gas compared to vent gas (type IIb_{vg}) were found as well. C_2/C_3 ratios higher in type I_{ss} compared to type IIa gas (Table 2) indicate additional propane depletion in shallow sediments, as previously reported for shallow deposits of mud volcanoes in the Sorokin Trough (Stadnitskaia et al., 2008), possibly owing to its concurrent microbial consumption (Kniemeyer et al., 2007). However, as propane depletions due to size exclusion during hydrate precipitations are also known (Milkov et al., 2004), the specific effects of the aforementioned abiotic and biotic processes leading to propane removal are uncertain. Biodegradation of ethane, however, could not be verified, as trends in $^{13}C/^{12}C$ isotopic ratios are vague and ethane fractions were highest in sedimentary gases (types I_{ss} and IIa_{ds}; Table 3).

Nevertheless, traces of *iso*-C_4 in some type I_{ss} and IIa_{ds} gases, as well as the presence of propane throughout all gas types demonstrate incomplete biodegradation. If taking place, production of secondary methane should proceed already in gas accumulations fueling the vent gas, as no trends in $\delta^{13}C$–CH_4 between vent gas (type IIb_{vg}) and type IIa_{ds} were observed. Biodegradation of LMWHC is considered to occur at temperatures below approx. 80 °C (Wilhelms et al., 2001), which in the Batumi subsurface might prevail not deeper than about 2.4 km bsf.

5.2.2.2. Methane consumption and production in shallow sediments. From shallow sediments, methane is typically lost by advection and diffusion into the water column and by consumption through AOM (Barnes and Goldberg, 1976; Reeburgh, 1976). Present AOM in Batumi top sediments is indicated by methane depletions relative to higher LMWHC along with enrichments in carbon dioxide in type I_{ss} gas compared to type IIa gas (Table 2; Fig. 4; see also Section 5.2.2.1). Haeckel et al. (2008) modeled that the AOM zone at the Batumi seep area is currently restricted to the upper tens of centimeters and during this study methane-derived authigenic carbonates indicating horizons of (sub)recent AOM were predominantly recovered from Units 1 and 2 in 90 cm bsf and above (Fig. 3).

Typically, AOM leads to ^{13}C-enrichments of the residual methane (Alperin et al., 1988; Whiticar, 1999; Ussler and Paull, 2008). Therefore, slightly more negative $\delta^{13}C$–CH_4 values in type I_{ss} gas compared to type II gases (−52.2‰ vs. −51.5‰ to −50.8‰; Table 3; Fig. 5b) along with highest fractions of methane–radiocarbon (0.6 to 1.4 pMC; Table 3; Fig. 6) provide evidence for methanogenesis in Batumi surface sediments. Methanogenesis in sulfate-bearing sediments was previously verified in the Pacific Ocean (Parkes et al., 2005), in the Gulf of Mexico (Orcutt et al., 2005, 2008), and in the Northwestern Black Sea (Knab et al., 2008), as well as during in vitro studies on AOM-performing microbial consortia under the presence of methane and sulfate (Seifert et al., 2006; Treude et al., 2007). Therefore, we conclude that AOM in surface sediments of the Batumi seep area is

spatially accompanied by microbial formation of ^{13}C-depleted methane, which in type I_{ss} gas over-compensates a general ^{13}C-enrichement in methane left from the AOM. In addition, highest ^{14}C–CH_4 contents were found for type I_{ss} gas released from DAPC cores (Fig. 6), which were recovered aside from areas of focused gas expulsion and contained not any or comparably low portions of Unit 3 sediments. Diffusive downward flux of ^{14}C–CH_4 from the water column or overlying sediments into Unit 3 is unlikely with respect to the gas ebullition intensity observed at the Batumi seep seafloor, gas fluxes calculated (Haeckel et al., 2008), and strong differences in isotopic compositions of methane dissolved in water masses of the respective depth range (δ^2H–CH_4 values ~ −130 to −100‰; Kessler et al., 2006a,b; ^{14}C contents ~ 9 to 15 pMC; Kessler et al., 2006a). Moreover, lowest and highest ^{14}C–CH_4 contents were found for samples recovered with the GBS and the DAPC, respectively, for which intrusion of seawater amounts during the sampling procedure in principle cannot be excluded, and ^{14}C contents in hydrate-bound methane (from intact hydrate pieces) compare well to methane in type IIa_{ds} gas (from pressure cores). This implies that methane in Units 1 and 2 is in fact rich in ^{12}C and ^{14}C but present only in comparably low abundances.

^{13}C–CO_2 enrichments in type I_{ss} and type IIa gases compared to that in vent gas (IIb_{vg}; Table 3) and water column-derived carbon dioxide (δ^{13}C–$CO_2 \approx -15.5$‰; Neretin et al., 2007), in conjunction with relative carbon dioxide depletions (Table 2; Fig. 4) and highest carbon isotope separations $\Delta\delta^{13}$C (CO_2–CH_4) (Table 3) hint at in situ bicarbonate methanogenesis in the depth interval between seafloor and the upper hydrate boundary. Bicarbonate-based methanogenesis was already reported for Black Sea methanotrophic mats (Treude et al., 2007) and sediment incubations (Knab et al., 2008), but as multiple processes influence ΣCO_2 in shallow sediments, the methanogenic pathways remain uncertain based on our data set.

5.3. Vertical distribution of subsurface gas hydrates

As demonstrated in Section 5.1, hydrate dissociation is not the basic cause of gas venting from the seafloor in ~840 m water depth. The presence of shallow-buried gas hydrates and intense discharge of free gas from the sea bottom indicate that LMWHC co-occur in different phases at the Batumi seep area. However, according to our phase calculations, this area is well located within the GHSZ (Fig. 7). Only a rise in bottom water temperatures by about 1.6 °C, a decrease in hydrostatic pressure by about 14 bar, or a combination of both would induce dissociation of shallow hydrates. Although seabottom pressure–temperature conditions of Black Sea bottom waters differing from present state are known from ancient (e.g., glacial, interglacial) times (Bahr et al., 2008), changes in pressure–temperature conditions in the recent past are unlikely to have effected the hydrate stability at the Batumi seep area.

Inferred from the LMWHC composition, sI hydrate, which is known to incorporate more methane and ethane relative to structure II hydrates, but to exclude C_{3+} hydrocarbons to a great extent (Sloan and Koh, 2007) is the dominant hydrate structure in Unit 3 sediments. Different LMWHC compositions in gas from pressure cores essentially restricted to Unit 1 and 2 sediments (type I_{ss}) and in those additionally containing Unit 3 (type IIa_{ds}) indicate preferential hydrate accumulations in Unit 3 and to a lesser extent in Unit 2.

The relationship found for hydrate distributions and individual lithologies might be explained by multiple mechanisms. The apparent lack of hydrates within Unit 1 deposits and in upper segments of Unit 2 most likely results from methane loss due to AOM in top sediments (Suess et al., 2001) and upward diffusion. Steep concentration gradients lead to upward diffusion of methane and strong depletions in upper Unit 2 material below the theoretical hydrate solubility. Nevertheless, AOM does not seem to occur in deeper Unit 2 sections, as hydrates were found in that depth range, but current sulfate penetration (Haeckel et al., 2008) and authigenic carbonate precipitates indicating (sub)recent AOM were restricted to Unit 1 in five out of eight carbonate-bearing cores.

Comparably low hydrate accumulations above Unit 3 appear also to be controlled by the lithological composition of the Batumi seep deposits. Massive hydrate layers in deeper sections of Unit 2 in GC 04, 08, and 18, were always spatially associated with aragonitic layers. This suggests that the prominent and comparably permeable aragonitic layers which create a maximum in TIC beyond the TOC-Peak (Fig. 3) could serve as lithological discontinuities which can be pushed apart in the course of hydrate crystallization.

5.4. Conceptual model of LMWHC partitioning in shallow Batumi seep sediments

To describe geo- and biochemical processes related to LMWHC migration and gas hydrate precipitation in surface sediments of the high-flux Batumi seep area, a conceptual model was developed (Fig. 8). Vent gas (type IIb_{vg}) containing a mixture of microbial and thermogenic LMWHC, which became biodegraded during ascend, is supplied through vertical faults from deep reservoirs into shallow sediments. This gas is dominated by radiocarbon-free, ^{13}C-enriched methane, followed by ethane and carbon dioxide and contains traces of C_{3+} hydrocarbons. Hydrates form as massive, isolated pieces in aragonitic layers in deeper Unit 2 sections and disseminated in Unit 3 sediments. These hydrates incorporate some part of the vent gas constituents with enrichments in methane and ethane and depletions in C_{3+} hydrocarbons and carbon dioxide to constitute type IIa gas. The majority of the vent gas escapes relatively unaltered with regard to chemistry and isotopy of its constituents into the water column.

Sea water-derived sulfate penetrates into surface sediments and promotes AOM to cause relative depletions in methane. Concomitant methanogenesis in top sediments leads to enrichments in ^{12}C–CH_4 and radiocarbon–methane of type I_{ss} gas. Diffusive transport into the water column due to concentration gradients and AOM lead to a decrease of in situ methane concentrations below the hydrate solubility in Unit 1 and in upper sections of Unit 2. Consequently, gas hydrates do not form in Unit 1 and within the top of Unit 2. Although the effects of biotic and abiotic LMWHC modifications are comparably small at the Batumi seep area, similar processes are likely to occur also at less active seepage areas in the Black Sea, which should be characterized by higher residence times within distinct gas reservoirs and, thus, greater impacts on the molecular and isotopic properties.

6. Conclusions

Autoclave technologies were used to collect natural gas and sediment samples from a high-flux hydrocarbon seep area in the permanently anoxic Eastern Black Sea basin. Gas chemical analysis of vent gas, shallow hydrates and pressure core gas from the Batumi seep area allowed characterizing multiple processes affecting partitioning and alteration of LMWHC and carbon dioxide, associated to gas migration in sediments, hydrate crystallization, microbial degradation and de novo formation of individual volatiles.

The major findings of this study are summarized as follows:

- LMWHC in the different gas types are predominantly fueled by microbial bicarbonate-based methanogenesis and to a lesser extent by thermocatalytic processes converting fossil, radiocarbon-free organic matter. Relative methane depletions along with enrichments in higher (thermogenic) homologues in vent gas contrast the LMWHC distributions in hydrate-bound gas and corroborate the assumption that vent gas is sourced from the deeper subsurface rather than from decomposing, shallow hydrates.
- Hydrates fueled by vent gas accumulate in deeper (i.e., approx. 90 cm bsf) sediment sections due to hydrocarbon supersaturation.

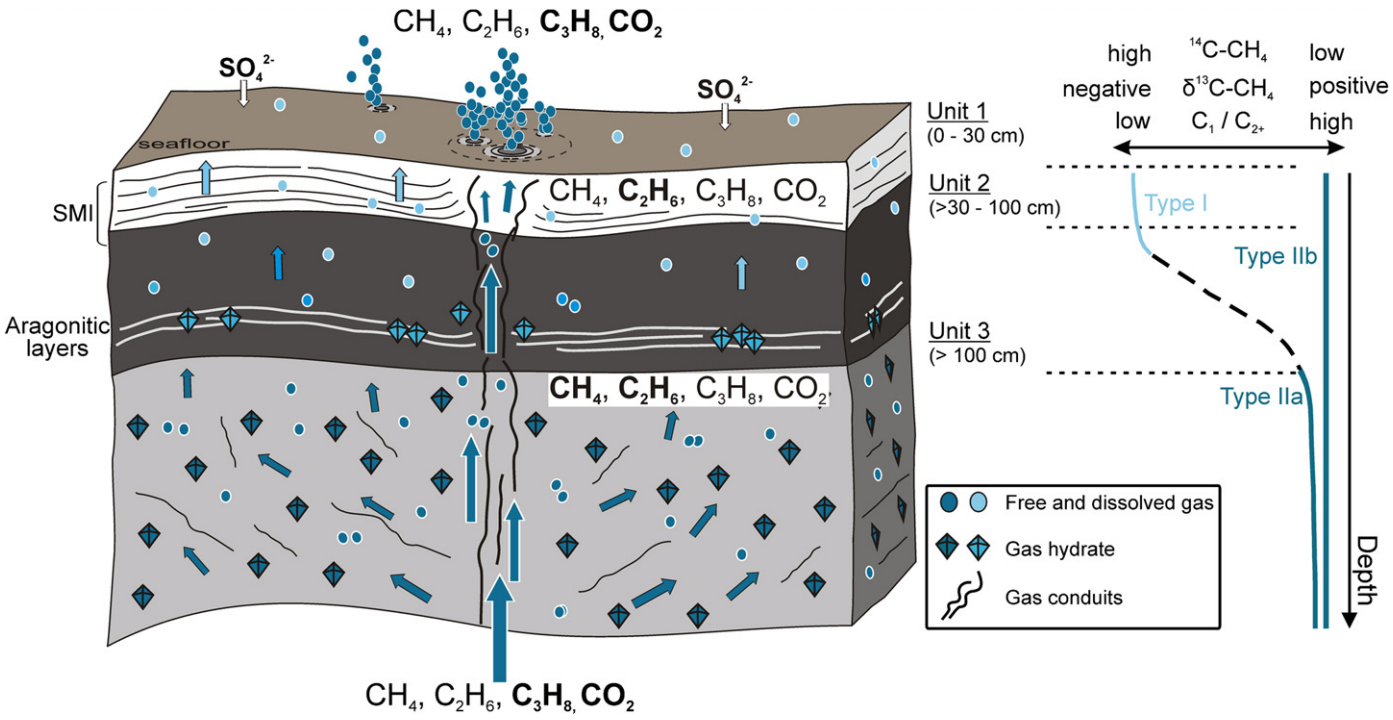

Fig. 8. Conceptual gas model (not to scale) for the different gas reservoirs in shallow deposits at the Batumi seep area. Average sediment thicknesses were calculated using specific thicknesses in gravity and pressure cores. Bold letters indicate relative enrichments of individual volatiles in specific gas samples (see Fig. 4). SMI = sulfate–methane-interface.

Enrichments in methane but depletions in ethane and carbon dioxide in near-surface pressure core gases relative to vent gas signify molecular partitioning during sI hydrate precipitation in shallow sediments. Contrarily, clear indications for isotopic fractionation of carbon and hydrogen during incorporation of LMWHC into the hydrates were lacking.

- Relative methane depletions of 0.03 mol.% of $\sum(C_1–C_4, CO_2)$ in gas from short cores (top sediments) compared to gas in longer cores are due to the anaerobic oxidation of methane (AOM). (Sub)recent AOM in Batumi seep deposits is substantiated by the presence of authigenic carbonates in Units 1 and 2 in 90 cm bsf and above.
- The presence of radiocarbon–methane (1.4 pMC) and enrichments in $^{12}C–CH_4$ found in comparably short sediment cores indicate the presence of methanogenesis converting fresh organic matter in shallow sediments.
- Anaerobic biodegradation of non-methane LMWHC already in the deep subsurface is indicated by *i*-C_4 over *n*-C_4 prevalence (up to 2.8) in vent gas, while propane consumption is substantiated by relative depletions along with ^{13}C-enrichments in sediments comprising Units 1 and 2.
- The high-flux Batumi seep area provides excellent opportunities for future studies on migration processes in the deep subsurface, on spatial distributions of near-surface gas hydrates, and on their dynamic behavior. In this context the area could serve as a model structure for high-flux hydrocarbon seepages within the GHSZ not only in the Black Sea but also elsewhere.

Acknowledgements

We gratefully thank the captain and crew of the R/V METEOR as well as the ROV 'QUEST 4000 m' team (MARUM, Bremen) for their excellent support during cruise M72/3. H.-J. Hohnberg is greatly acknowledged for design and preparation of autoclave tools and deployments of the DAPC. A.H. Mai and K. Dehning (MARUM) are thanked for technical support during preparation of DAPC deployments. E. Kozlova (MSU, Russia) is acknowledged for performing visual core descriptions during M72 Leg 3a and S. Kusch (AWI, Bremerhaven) for support during the degassing experiments and onboard gas analysis during M72 Leg 3b. H. Buschhoff (MARUM) performed CN analyses. K. Stange (IFM-Geomar, Kiel) is thanked for some stable carbon isotope measurements on methane and X. Prieto-Mollar and M. Elvert (both MARUM) are thanked for analytical support during stable carbon isotope measurements of low-molecular-weight hydrocarbons.

This paper has benefited considerably from the constructive comments from J.-L. Charlou and from an anonymous reviewer. This is contribution GEOTECH-1302 of the R&D program GEOTECHNOLOGIEN funded by the German Ministry of Education and Research (BMBF) and the German Research Foundation (DFG), collaborative project METRO (grant 03G0604A) and through DFG-Research Center/Excellence Cluster "The Ocean in the Earth System".

References

Abegg, F., Hohnberg, H.J., Pape, T., Bohrmann, G., Freitag, J., 2008. Development and application of pressure-core-sampling systems for the investigation of gas- and gas-hydrate-bearing sediments. Deep Sea Research Part I: Oceanographic Research Papers 55 (11), 1590–1599.

Aloisi, G., Wallmann, K., Drews, M., Bohrmann, G., 2004. Evidence for the submarine weathering of silicate minerals in Black Sea sediments: possible implications for the marine Li and B cycles. Geochemistry Geophysics Geosystems 5 (4), Q04007. doi:10.1029/2003GC000639.

Alperin, M.J., Reeburgh, W.S., Whiticar, M.J., 1988. Carbon and hydrogen isotope fractionation resulting from anaerobic methane oxidation. Global Biogeochemical Cycles 2 (3), 279–288.

Bahr, A., Lamy, F., Arz, H.W., Major, C., Kwiecien, O., Wefer, G., 2008. Abrupt changes of temperature and water chemistry in the late Pleistocene and early Holocene Black Sea. Geochemistry Geophysics Geosystems 9 (1), Q01004.

Banks, C.J., Robinson, A.G., Williams, A.P., 1997. Structure and regional tectonic of the Achara–Trialet Fold Belt and the adjacent Rioni and Kartli Foreland Basins, Republic of Georgia. In: Robinson, A.G. (Ed.), Regional and petroleum geology of the Black Sea and surrounding region. The American Association of Petroleum Geologists Memoir.

Barnes, R.O., Goldberg, E.D., 1976. Methane production and consumption in anaerobic marine sediments. Geology 4 (5), 297–300.

Beal, E.J., House, C.H., Orphan, V.J., 2009. Manganese- and iron-dependent marine methane oxidation. Science 325 (5937), 184–187.

Bernard, B.B., Brooks, J.M., Sackett, W.M., 1976. Natural gas seepage in the Gulf of Mexico. Earth and Planetary Science Letters 31 (1), 48–54.

Bhatnagar, G., Chapman, W.G., Dickens, G.R., Dugan, B., Hirasaki, G.J., 2008. Sulfate–methane transition as a proxy for average methane hydrate saturation in marine sediments. Geophysical Research Letters 35, L03611. doi:10.1029/2007GL032500.

Blinova, V., Ivanov, M., Bohrmann, G., 2003. Hydrocarbon gases in deposits from mud volcanoes in the Sorokin Trough, north-eastern Black Sea. Geo-Marine Letters 23 (3–4), 250–257.

Bohrmann, G., Ivanov, M., Foucher, J.-P., Spiess, V., Bialas, J., Greinert, J., Weinrebe, W., Abegg, F., Aloisi, G., Artemov, Y., Blinova, V., Drews, M., Heidersdorf, F., Krabbenhöft, A., Klaucke, I., Krastel, S., Leder, T., Polikarpov, I., Saburova, M., Schmale, O., Seifert, R., Volkonskaya, A., Zillmer, M., 2003. Mud volcanoes and gas hydrates in the Black Sea: new data from Dvurechenskii and Odessa mud volcanoes. Geo-Marine Letters 23 (3–4), 239–249.

Bohrmann, G., Pape, T., and cruise participants, 2007. Report and preliminary results of R/V Meteor cruise M72/3, Istanbul–Trabzon–Istanbul, 17 March – 23 April, 2007. Marine gas hydrates of the Eastern Black Sea, Bremen.

Boreham, C.J., Edwards, D.S., Hope, J.M., Chen, J., Hong, Z., 2008. Carbon and hydrogen isotopes of neo-pentane for biodegraded natural gas correlation. Organic Geochemistry 39 (10), 1483–1486.

Borowski, W.S., Paull, C.K., Ussler III, W., 1996. Marine pore-water sulfate profiles indicate in situ methane flux from underlying gas hydrate. Geology 24 (7), 655–658.

Bourry, C., Chazallon, B., Charlou, J.L., Pierre Donval, J., Ruffine, L., Henry, P., Geli, L., Çagatay, M.N., Inan, S., Moreau, M., 2009. Free gas and gas hydrates from the Sea of Marmara, Turkey: chemical and structural characterization. Chemical Geology 264 (1–4), 197–206.

Brooks, J.M., Cox, H.B., Bryant, W.R., Kennicutt, M.C., Mann, R.G., McDonald, T.J., 1986. Association of gas hydrates and oil seepage in the Gulf of Mexico. Organic Geochemistry 10 (1–3), 221–234.

Charlou, J.L., Donval, J.P., Bourry, C., Chaduteau, C., Lanteri, N., Bignon, L., Foucher, J.P., Nouzé, H., and the VICKING Scientific team, 2007. Gas bubbles and gas hydrates sampling from Hakon Mosby Mud Volcano – preliminary results – VICKING cruise (2006). Geophysical Research Abstracts 9, 08690.

Claypool, G.E., Kvenvolden, K.A., 1983. Methane and other hydrocarbon gases in marine sediment. Annual Review of Earth and Planetary Sciences 11 (1), 299–327.

Clayton, C., 1991. Carbon isotope fractionation during natural gas generation from kerogen. Marine and Petroleum Geology 8 (2), 232–240.

Clayton, J.L., 1998. Geochemistry of coalbed gas — a review. International Journal of Coal Geology 35 (1–4), 159–173.

Dai, J., Song, Y., Dai, C., Wang, D., 1996. Geochemistry and accumulations of carbon dioxide gases in China. The American Association of Petroleum Geologists Bulletin 80 (10), 1615–1626.

Dumke, I., Faber, E., Poggenburg, J., 1989. Determination of stable carbon and hydrogen isotopes of light hydrocarbons. Analytical Chemistry 61 (19), 2149–2154.

Efendiyeva, M.A., 2004. Anoxia in waters of the Maikop paleobasin (Tethys Ocean, Azeri sector), with implications for the modern Caspian Sea. Geo-Marine Letters 24 (3), 177–181.

Feseker, T., Pape, T., Wallmann, K., Klapp, S.A., Schmidt-Schierhorn, F., Bohrmann, G., 2009. The thermal structure of the Dvurechenskii mud volcano and its implications for gas hydrate stability and eruption dynamics. Marine and Petroleum Geology 26 (9), 1812–1823.

Ginsburg, G.D., Soloviev, V.A., 1997. Methane migration within the submarine gas-hydrate stability zone under deep-water conditions. Marine Geology 137 (1–2), 49–57.

Haeckel, M., Suess, E., Wallmann, K., Rickert, D., 2004. Rising methane gas bubbles form massive hydrate layers at the seafloor. Geochimica et Cosmochimica Acta 68 (21), 4335–4345.

Haeckel, M., Reitz, A., Klaucke, I., 2008. Methane budget of a large gas hydrate province offshore Georgia, Black Sea, 6th International Conference on Gas hydrates (ICGH). Vancouver, British Columbia.

Head, I.M., Jones, D.M., Larter, S.R., 2003. Biological activity in the deep subsurface and the origin of heavy oil. Nature 426 (6964), 344–352.

Heeschen, K.U., Hohnberg, H.J., Haeckel, M., Abegg, F., Drews, M., Bohrmann, G., 2007. In situ hydrocarbon concentrations from pressurized cores in surface sediments, Northern Gulf of Mexico. Marine Chemistry 107 (4), 498–515.

Hinrichs, K.-U., Boetius, A., 2002. The anaerobic oxidation of methane: new insights in microbial ecology and biogeochemistry. In: Wefer, G., Billet, D., Hebbeln, D., Jørgensen, B.B., Schlüter, M., van Weering, T.C.E. (Eds.), Ocean Margin Systems. Springer-Verlag, Heidelberg, pp. 457–477.

Hoehler, T.M., Alperin, M.J., Albert, D.B., Martens, C.S., 1994. Field and laboratory studies of methane oxidation in an anoxic marine sediment: evidence for a methanogen–sulfate reducer consortium. Global Biogeochemical Cycles 8 (4), 451–463.

Horstad, I., Larter, S.R., 1997. Petroleum migration, alteration, and remigration within Troll field, Norwegian North Sea. The American Association of Petroleum Geologists Bulletin 81 (2), 222–248.

Inan, S., Namik Yalçin, M., Guliev, I.S., Kuliev, K., Akper Feizullayev, A., 1997. Deep petroleum occurrences in the Lower Kura Depression, South Caspian Basin, Azerbaijan: an organic geochemical and basin modeling study. Marine and Petroleum Geology 14 (7–8), 731–762.

Irwin, H., Curtis, C.D., Coleman, M., 1977. Isotopic evidence for source of diagenetic carbonates formed during burial of organic rich sediments. Nature 269 (5625), 209–213.

James, A.T., Burns, B.J., 1984. Microbial alteration of subsurface natural gas accumulations. The American Association of Petroleum Geologists Bulletin 68 (8), 957–960.

Jones, D.M., Head, I.M., Gray, N.D., Adams, J.J., Rowan, A.K., Aitken, C.M., Bennett, B., Huang, H., Brown, A., Bowler, B.F.J., Oldenburg, T., Erdmann, M., Larter, S.R., 2008. Crude-oil biodegradation via methanogenesis in subsurface petroleum reservoirs. Nature 451 (7175), 176–180.

Jørgensen, B.B., Weber, A., Zopfi, J., 2001. Sulfate reduction and anaerobic methane oxidation in Black Sea sediments. Deep-Sea Research I 48, 2097–2120.

Judd, A.G., Hovland, M., Dimitrov, L.I., Garcia Gil, S., Jukes, V., 2002. The geological methane budget at Continental Margins and its influence on climate change. Geofluids 2 (2), 109–126.

Kessler, J.D., Reeburgh, W.S., 2005. Preparation of natural methane samples for stable isotope and radiocarbon analysis. Limnology and Oceanography Methods 3, 408–418.

Kessler, J.D., Reeburgh, W.S., Southon, J., Seifert, R., Michaelis, W., Tyler, S.C., 2006a. Basin-wide estimates of the input of methane from seeps and clathrates to the Black Sea. Earth and Planetary Science Letters 243 (3–4), 366–375.

Kessler, J.D., Reeburgh, W.S., Tyler, S.C., 2006b. Controls on methane concentration and stable isotope (δ^2H–CH$_4$ and δ^{13}C–CH$_4$) distributions in the water columns of the Black Sea and Cariaco Basin. Global Biogeochemical Cycles 20, GB4004. doi:10.1029/2005TGB002571.

Klaucke, I., Sahling, H., Weinrebe, W., Blinova, V., Bürk, D., Lursmanashvili, N., Bohrmann, G., 2006. Acoustic investigation of cold seeps offshore Georgia, eastern Black Sea. Marine Geology 231 (1–4), 51–67.

Knab, N.J., Cragg, B.A., Hornibrook, E.R.C., Holmkvist, L., Borowski, C., Parkes, R.J., Jørgensen, B.B., 2008. Regulation of anaerobic methane oxidation in sediments of the Black Sea. Biogeosciences 6, 1505–1518.

Kniemeyer, O., Musat, F., Sievert, S.M., Knittel, K., Wilkes, H., Blumenberg, M., Michaelis, W., Classen, A., Bolm, C., Joye, S.B., Widdel, F., 2007. Anaerobic oxidation of short-chain hydrocarbons by marine sulphate-reducing bacteria. Nature 449 (7164), 898–901.

Lamy, F., Arz, H.W., Bond, G.C., Bahr, A., Pätzold, J., 2006. Multicentennial-scale hydrological changes in the Black Sea and northern Red Sea during the Holocene and the Arctic/North Atlantic Oscillation. Paleoceanography 21, PA1008. doi:10.1029/2005PA001184.

Larter, S., di Primio, R., 2005. Effects of biodegradation on oil and gas field PVT properties and the origin of oil rimmed gas accumulations. Organic Geochemistry 36 (2), 299–310.

Meredith, D.J., Egan, S.S., 2002. The geological and geodynamic evolution of the eastern Black Sea basin: insights from 2-D and 3-D tectonic modelling. Tectonophysics 350 (2), 157–179.

Milkov, A.V., 2005. Molecular and stable isotope compositions of natural gas hydrates: a revised global dataset and basic interpretations in the context of geological settings. Organic Geochemistry 36 (5), 681–702.

Milkov, A.V., Dzou, L., 2007. Geochemical evidence of secondary microbial methane from very slight biodegradation of undersaturated oils in a deep hot reservoir. Geology 35 (5), 455–458.

Milkov, A.V., Claypool, G.E., Lee, Y.-J., Torres, M.E., Borowski, W.S., Tomaru, H., Sassen, R., Long, P.E., Leg, O.D.P., 204 Scientific Party, 2004. Ethane enrichment and propane depletion in subsurface gases indicate gas hydrate occurrence in marine sediments at southern Hydrate Ridge offshore Oregon. Organic Geochemistry 35 (9), 1067–1080.

Müller, P.J., Schneider, R.R., Ruhland, G., 1994. Late Quaternary pCO_2 variations in the Angola Current: evidence from organic carbon δ^{13}C and alkenone temperatures. In: Zahn, R. (Ed.), Constraints on the Ocean's Role in Global Change. Springer-Verlag, Carbon Cycling in the Glacial Ocean, pp. 343–366.

Naudts, L., Greinert, J., Artemov, Y., Staelens, P., Poort, J., Van Rensbergen, P., De Batist, M., 2006. Geological and morphological setting of 2778 methane seeps in the Dnepr paleo-delta, northwestern Black Sea. Marine Geology 227 (3–4), 177–199.

Neretin, L.N., Abed, R.M.M., Schippers, A., Schubert, C.J., Kohls, K., Kuypers, M.M.M., 2007. Inorganic carbon fixation by sulfate-reducing bacteria in the Black Sea water column. Environmental Microbiology 9 (12), 3019–3024.

Nikolovska, A., Sahling, H., Bohrmann, G., 2008. Novel hydro-acoustic methodology for detection, localization and quantification of gas bubbles rising from the seafloor at gas seeps from the eastern Black Sea. Geochemistry Geophysics Geosystems (G3) 9 (10), Q10010. doi:10.1029/2008GC002118.

Orcutt, B., Boetius, A., Elvert, M., Samarkin, V., Joye, S.B., 2005. Molecular biogeochemistry of sulfate reduction, methanogenesis and the anaerobic oxidation of methane at Gulf of Mexico cold seeps. Geochimica et Cosmochimica Acta 69 (17), 4267–4281.

Orcutt, B., Samarkin, V., Boetius, A., Joye, S., 2008. On the relationship between methane production and oxidation by anaerobic methanotrophic communities from cold seeps of the Gulf of Mexico. Environmental Microbiology 10 (5), 1108–1117.

Orphan, V.J., Taylor, L.T., Hafenbradl, D., Delong, E.F., 2000. Culture-dependent and culture-independent characterization of microbial assemblages associated with high-temperature petroleum reservoirs. Applied and Environmental Microbiology 66 (2), 700–711.

Pallasser, R.J., 2000. Recognising biodegradation in gas/oil accumulations through the δ^{13}C compositions of gas components. Organic Geochemistry 31 (12), 1363–1373.

Pape, T., Blumenberg, M., Seifert, R., Bohrmann, G., Michaelis, W., 2008. Marine methane biogeochemisty of the Black Sea: a review. In: Dilek, Y., Furnes, H., Muehlenbachs, K. (Eds.), Links Between Geological Processes, Microbial Activities & Evolution of Life. Springer Science + Business Media B.V.

Parkes, R.J., Webster, G., Cragg, B.A., Weightman, A.J., Newberry, C.J., Ferdelman, T.G., Kallmeyer, J., Jørgensen, B.B., Aiello, I.W., Fry, J.C., 2005. Deep sub-seafloor prokaryotes stimulated at interfaces over geological time. Nature 436 (7049), 390–394.

Pohlman, J.W., Canuel, E.A., Chapman, N.R., Spence, G.D., Whiticar, M.J., Coffin, R.B., 2005. The origin of thermogenic gas hydrates on the northern Cascadia Margin as inferred from isotopic (^{13}C/^{12}C and D/H) and molecular composition of hydrate and vent gas. Organic Geochemistry 36 (5), 703–716.

Prinzhofer, A., Pernaton, E., 1997. Isotopically light methane in natural gas: bacterial imprint or diffusive fractionation? Chemical Geology 142 (3–4), 193–200.

Prinzhofer, A.A., Huc, A.Y., 1995. Genetic and post-genetic molecular and isotopic fractionations in natural gases. Chemical Geology 126 (3–4), 281–290.

Raghoebarsing, A.A., Pol, A., van de Pas-Schoonen, K.T., Smolders, A.J.P., Ettwig, K.F., Rijpstra, W.I.C., Schouten, S., Sinninghe Damsté, J.S., Op den Camp, H.J.M., Jetten, M.S.M., Strous, M., 2006. A microbial consortium couples anaerobic methane oxidation to denitrification. Nature 440 (7086), 918–921.

Reeburgh, W.S., 1976. Methane consumption in Cariaco Trench waters and sediments. Earth and Planetary Science Letters 28 (3), 337–344.

Reeburgh, W.S., Ward, B.B., Whalen, S.C., Sandbeck, K.A., Kilpatrick, K.A., Kerkhof, L.J., 1991. Black Sea methane geochemistry. Deep-Sea Research 38 (Suppl. 2), S1189–S1210.

Rice, D.D., Claypool, G.E., 1981. Generation, accumulation, and resource potential of biogenic gas. The American Association of Petroleum Geologists Bulletin 65 (1), 5–25.
Rooney, M.A., Claypool, G.E., Chung, H.M., 1995. Modeling thermogenic gas generation using carbon isotope ratios of natural gas hydrocarbons. Chemical Geology 126 (3–4), 219–232.
Ross, D.A., Degens, E.T., 1974. Recent sediments of Black Sea. In: Degens, E.T., Ross, D.A. (Eds.), The Black Sea — Geology, Chemistry and Biology. The American Association of Petroleum Geologists, Tusla, USA.
Sassen, R., Joye, S., Sweet, S.T., de Freitas, D.A., Milkov, A.V., MacDonald, I.R., 1999. Thermogenic gas hydrates and hydrocarbon gases in complex chemosynthetic communities, Gulf of Mexico continental slope. Organic Geochemistry 30 (7), 485–497.
Sassen, R., Sweet, S.T., DeFreitas, D.A., Milkov, A.V., 2000. Exclusion of 2-methylbutane (isopentane) during crystallization of structure II gas hydrate in sea-floor sediment, Gulf of Mexico. Organic Geochemistry 31 (11), 1257–1262.
Sassen, R., Sweet, S.T., Milkov, A.V., DeFreitas, D.A., Kennicutt II, M.C., 2001. Thermogenic vent gas and gas hydrate in the Gulf of Mexico slope: is gas hydrate decomposition significant? Geology 29 (2), 107–110.
Sassen, R., Milkov, A.V., Ozgul, E., Roberts, H.H., Hunt, J.L., Beeunas, M.A., Chanton, J.P., DeFreitas, D.A., Sweet, S.T., 2003. Gas venting and subsurface charge in the Green Canyon area, Gulf of Mexico continental slope: evidence of a deep bacterial methane source? Organic Geochemistry 34 (10), 1455–1464.
Sassen, R., Roberts, H.H., Carney, R., Milkov, A.V., DeFreitas, D.A., Lanoil, B., Zhang, C., 2004. Free hydrocarbon gas, gas hydrate, and authigenic minerals in chemosynthetic communities of the northern Gulf of Mexico continental slope: relation to microbial processes. Chemical Geology 205 (3–4), 195–217.
Schoell, M., 1980. The hydrogen and carbon isotopic composition of methane from natural gases of various origins. Geochimica et Cosmochimica Acta 44 (5), 649–661.
Schoell, M., 1983. Genetic characterization of natural gases. The American Association of Petroleum Geologists Bulletin 67 (12), 2225–2238.
Schoell, M., 1988. Multiple origins of methane in the earth. Chemical Geology 71 (1–3), 1–10.
Scott, A.R., Kaiser, W.R., Ayers, W.B., 1994. Thermogenic and secondary biogenic gases, San Juan Basin, Colorado and New Mexico—implications for coalbed gas producibility. The American Association of Petroleum Geologists Bulletin 78 (8), 1186–1209.
Seewald, J.S., 2003. Organic–inorganic interactions in petroleum-producing sedimentary basins. Nature 426 (6964), 327–333.
Seifert, R., Nauhaus, K., Blumenberg, M., Krüger, M., Michaelis, W., 2006. Methane dynamics in a microbial community of the Black Sea traced by stable carbon isotopes *in vitro*. Organic Geochemistry 37 (10), 1411–1419.
Sloan, E.D., Koh, C.A., 2007. Clathrate hydrates of natural gases. CRC Press, Boca Raton.
Stadnitskaia, A., Ivanov, M.K., Blinova, V., Kreulen, R., van Weering, T.C.E., 2006. Molecular and carbon isotopic variability of hydrocarbon gases from mud volcanoes in the Gulf of Cadiz, NE Atlantic. Marine and Petroleum Geology 23 (3), 281–296.
Stadnitskaia, A., Ivanov, M.K., Poludetkina, E.N., Kreulen, R., van Weering, T.C.E., 2008. Sources of hydrocarbon gases in mud volcanoes from the Sorokin Trough, NE Black Sea, based on molecular and carbon isotopic compositions. Marine and Petroleum Geology 25 (10), 1040–1057.
Stuiver, M., Polach, H.A., 1977. Reporting of ^{14}C data. Radiocarbon 19 (3), 355–363.
Suess, E., Torres, M., Bohrmann, G., Collier, R.W., Greinert, J., Linke, P., Rehder, G., Tréhu, A., Wallmann, K., Winckler, G., Zuleger, E., 1999. Gas hydrate destabilization: enhanced dewatering, benthic material turnover and large methane plumes at the Cascadia convergent margin. Earth and Planetary Science Letters 170, 1–15.
Suess, E., Torres, M., Bohrmann, G., Collier, R.W., Rickert, D., Goldfinger, C., Linke, P., Heuser, A., Sahling, H., Heeschen, K., Jung, C., Nakamura, K., Greinert, J., Pfannkuche, O., Tréhu, A., Klinkhammer, G., Whiticar, M.J., Eisenhauer, A., Teichert, B., Elvert, M., 2001. Sea floor methane hydrates at Hydrate Ridge, Cascadia Margin. In: Paull, C.K., Dillon, W.P. (Eds.), Natural gas hydrates — Occurrences, Distribution and Detection. AGU Monograph Washington.
Treude, T., Orphan, V., Knittel, K., Gieseke, A., House, C.H., Boetius, A., 2007. Consumption of methane and CO_2 by methanotrophic microbial mats from gas seeps of the anoxic Black Sea. Applied and Environmental Microbiology 73 (7), 2271–2283.
Ussler III, W., Paull, C.K., 2008. Rates of anaerobic oxidation of methane and authigenic carbonate mineralization in methane-rich deep-sea sediments inferred from models and geochemical profiles. Earth and Planetary Science Letters 266 (3–4), 271–287.
Valentine, D.L., Chidthaisong, A., Rice, A., Reeburgh, W.S., Tyler, S.C., 2004. Carbon and hydrogen isotope fractionation by moderately thermophilic methanogens. Geochimica et Cosmochimica Acta 68 (7), 1571–1590.
Wagner-Friedrichs, M., 2007. Seafloor seepage in the Black Sea: mud volcanoes, seeps and diapiric structures imaged by acoustic methods. Ph.D. Thesis, University of Bremen, Bremen.
Whiticar, M.J., 1989. A geochemical perspective of natural gas and atmospheric methane. Organic Geochemistry 16 (1–3), 531–547.
Whiticar, M.J., 1999. Carbon and hydrogen isotope systematics of bacterial formation and oxidation of methane. Chemical Geology 161 (1–3), 291–314.
Whiticar, M.J., Faber, E., Schoell, M., 1986. Biogenic methane formation in marine and freshwater environments: CO_2 reduction *vs.* acetate fermentation — isotope evidence. Geochimica et Cosmochimica Acta 50 (5), 693–709.
Widdel, F., Rabus, R., 2001. Anaerobic biodegradation of saturated and aromatic hydrocarbons. Current Opinion in Biotechnology 12, 259–276.
Wilhelms, A., Larter, S.R., Head, I., Farrimond, P., di-Primio, R., Zwach, C., 2001. Biodegradation of oil in uplifted basins prevented by deep-burial sterilization. Nature 411 (6841), 1034–1037.
Wycherley, H., Fleet, A., Shaw, H., 1999. Some observations on the origins of large volumes of carbon dioxide accumulations in sedimentary basins. Marine and Petroleum Geology 16 (6), 489–494.
Zengler, K., Richnow, H.H., Rosselló-Mora, R., Michaelis, W., Widdel, F., 1999. Methane formation from long-chain alkanes by anaerobic microorganisms. Nature 401, 266–269.